TRIBHUVAN UNIVERSITY

INSTITUTE OF ENGINEERING

PULCHOWK CAMPUS

B-10-BME-2013/2017

Modeling of Gas-Phase Combustion with Detailed Reaction Mechanism and Study of Combustion Test Cases

by

Anish Acharya

Sagar Pokharel

Suman Subedi

Susan Lama

A PROJECT REPORT

SUBMITTED TO THE DEPARTMENT OF MECHANICAL ENGINEERING

IN PARTIAL FULFILLMENT OF THE REQUIREMENTS FOR THE

DEGREE OF BACHELOR IN MECHANICAL ENGINEERING

DEPARTMENT OF MECHANICAL ENGINEERING

LALITPUR, NEPAL

SEPTEMBER, 2017

COPYRIGHT

TRIBHUVAN UNIVERSITY

INSTITUTE OF ENGINEERING

PULCHOWK CAMPUS

DEPARTMENT OF MECHANICAL ENGINEERING

APPROVAL PAGE

The undersigned certify that they have read, and recommended to the Institute of Engineering for acceptance, a project report entitled " Modeling of Gas-Phase Combustion with Detailed Reaction Mechanism and Study of Combustion Test Cases " submitted by Anish Acharya , Sagar Pokharel, Suman Subedi and Susan Lama in partial fulfillment of the requirements for the degree of Bachelor of Mechanical Engineering.

_____

Supervisor, Asst. Prof. Sudip Bhattrai

Faculty

Department of Mechanical Engineering

_____

External Examiner, Mr. Hari Bahadur Dura

Faculty

Kathmandu University

_____

Committee Chairperson, Dr. Nawaraj Bhattrai

Head

Department of Mechanical Engineering

_____

Date

ABSTRACT

A mathematical model for Closed Homogeneous Constant Pressure Reactor (CHCPR) and one-dimensional Premixed Reactive Flow (PRFM) is developed for the thesis. Detailed gas phase reaction kinetics is coupled with thermodynamics and flow properties to develop the reactor models. Global reaction mechanisms are used for simulating combustion in complex flows. However, study of accurate combustion physics efficiently requires detailed chemical kinetics in simplified flow system as it gives more accurate results for studying ignition, explosion, reaction progression and other transient properties of flame. Detailed reaction mechanism with three Arrhenius rate parameters and third-body efficiencies are considered. Thermodynamic properties are calculated using the 7 coefficient NASA polynomials. CHCPR calculates the transient reaction properties like temperature, species concentration, volumetric heat release, etc., during the progression of reaction at constant pressure. PRFM solves both the reaction properties and flow properties like pressure and velocity along the length of the combustor. Addition of source terms in PRFM is considered to facilitate exchange of heat and mass from surrounding. Governing equations for the reactor models are derived in the form of a system of nonlinear Ordinary Differential Equations (ODEs), which are solved using ode15s for CHCPR and Backward Differentiation Newton-Raphson Method with Finite Difference Jacobian for PRFM.

To incorporate complex flow characteristics like laminar and turbulent mixing and transport properties in the combustion test cases, ANSYS Fluent is used. Preliminary design of the gas combustor includes, design of geometry for temperature control at exit for rated power. Calculation of the fuel mass flow rate for rated power in CHCPR and diluent mass flow rate for temperature control is done in PRFM. Physics behind the simple premixed flow, bluff body and cavity flame holding are studied in ANSYS Fluent.

ACKNOWLEDGEMENT

We would like to extend sincere thanks, first and foremost, to our project supervisor, Asst. Prof. Sudip Bhattrai, for his valuable suggestions and guidance through the project. His enthusiasm towards the science of combustion has been a continual source of inspiration for us in pursuing this field. Additionally, we would like to thank Mr. Bikalpa Bomjan for providing us the guidance during the course of the project.

We would also like to express our deep gratitude to Department of Mechanical Engineering, IOE, Pulchowk Campus for providing us opportunities and required resources throughout the bachelor's degree program. More so, we would like to thank Dr. Nawaraj Bhattrai, Head of Department for his support. Our thanks also goes to Mr. Rudra Mani Ghimire, Deputy Head of Department for his valuable suggestions on the project.

We would also like to thank our seniors and all our friends who helped us with their valuable suggestions.

TABLE OF CONTENTS

LIST OF TABLES

LIST OF FIGURES

LIST OF ABBREVIATIONS

NOx	Nitrogen Oxides
SOx	Sulphur Oxides
CO	Carbon monoxide
OTEC	Ocean Thermal Energy Conversion
CFD	Computational Fluid Dynamics
CHCPR	Closed Homogenous Constant Pressure Reactor
PRFM	Premixed Reactive Flow Model

LIST OF SYMBOLS

X_i	Mole Fraction
Y_i	Mass Fraction
N_i	No. of Moles
m_i	Mass of species i
MW	Molecular Weight
ρ	Density
$[X_i]$	Concentration of X_i
T	Temperature
E_a	Activation Energy
R	Universal Gas Constant
k	Rate Constant
K_P	Equilibrium constant
n	Order of Reaction
v	Velocity of the mixture
u	X-component of the velocity of the mixture
$\dot{\omega}_\iota$	Volumetric moles generation of the i^{th} species
V	Volume
H	Enthalpy
A_r	Pre-exponential factor
C_p	Molar Constant Pressure Heat Capacity
c_p	Constant Pressure Specific Heat Capacity
$\dot{Q}''$	Heat flux outflow from wall
$\wp$	Perimeter of the reactor
tr	Residence time
q_v	Rate of Heat Production

CHAPTER ONE: INTRODUCTION

1.1 Background

The invention of fire is an important factor, marking the dawn of human civilization. Coming to the modern era, today, people use fire for heating, lighting and as a source of energy for various means of transportation. Wildfires and urban fire cause a tremendous amount of loss of life and property. The pollutants from combustion like NOx, CO, CO2, SOx cause various harmful effects to the environment. So, combustion is certainly a branch of science that affects almost every aspect of human activities.

Though there are a large variety of alternative energy sources available such as nuclear, solar, wind, hydroelectric, geothermal, and OTEC, chemical energy derived from burning fossil fuels supplies a disproportionately large fraction of the total world energy needs. Combustion converts 78.4% of world energy (IEA, 2014) and has played a dominant role in ground and air transportation. With the current difficulties in developing renewable energy, for a foreseeable future, the design and operation of heat and power devices is closely related to the issue of efficient energy utilization.

Combustion systems primarily comprise the physical processes of thermodynamics, chemical kinetics and fluid dynamics. Thermodynamics of the reactive fluid include microscopic heat transfer between gas molecules, work done by pressure, and the associated volume change. Chemical kinetics determine the generation/consumption of chemical species under the constraint of mass conservation. Thermodynamics and chemical kinetics combined gives the equilibrium and energy release or consumed. Temporal change and spatial convection of the flow properties due to conservation of mass, momentum, and energy is governed by fluid dynamics. Combustion in various systems involves a number of time and length scales, that for example, defines the time and length required for completion of reaction in a relevant combustion system, is affected by the interaction of molecules at atomic level, molecular diffusion, soot particle formation, phase change of working substance, simultaneous mixing, property of fuel and various other factors. Thus, the multidisciplinary field of combustion presents a challenge to develop the required combustion modeling approach which can address

multi-physical combustion processes accurately with detailed chemical kinetic mechanisms.

Atomization, vaporization, gas phase mixing and chemical reaction takes place during combustion process. The slower reaction step control combustion efficiency. Therefore, the knowledge of completion time for the various steps and the overall combustion time is necessary. Vaporization is often the slowest, rate controlling step. Gas phase mixing may also be a slow step. Often, chemical reactions take place infinitely fast in comparison with other steps and are neglected but this assumption may not always be valid. (Hersch, 1967)

The need for the energy conservation and pollution reduction has led to increased study of kinetically controlled chemical reactions in the combustion processes. In energy associated research, if a set of realistic kinetic steps is given, simulation of combustion processes could be studied by a variation of input parameters to find the conditions that would provide optimum extraction of energy from a fuel. In pollution research, the conditions where pollutant levels would be reduced could be studied with some insurance that the predicted changes would actually result. (Mclain & Rao, 1976)

Descriptions of combustion processes, at the level of the elementary chemical steps that occur, on the basis of their individual rate parameters, have enjoyed notable advance in recent years through the development of a variety of detailed chemical-kinetic mechanism (Petrova & Williams, 2006).

Proper combustion modeling with detailed chemical kinetics will enable study of renewable fuels and fuel blends to be integrated with existing technologies along with control of pollutants from combustion emission. These outcomes clearly highlight the richness of the possible avenues that can be explored for development of efficient combustion systems. The knowledge of chemical equilibrium compositions of chemical system can be applied to a wide variety of problems in chemistry and chemical engineering (Battin-Leclerc et al., 2011). Some applications are design and analysis of equipment such as compressors, turbines, nozzles, engines, shock tubes, heat exchangers, etc.

1.2 Problem statement

In modelling of a combustion system, infinite rate chemical reaction greatly simplifies the problem but at a cost of huge error in calculation as combustion efficiency is neglected. Currently the design approach is based on general experience and experimental results lacking a proper mathematical model and/or methodology which incorporates both mixing and combustion. Also, global reaction chemistry models are good choice but they are only acceptable for limited operated ranges and cannot account for all of the possible combustion phenomena like auto ignition, heat release, $NO_{x,}$ etc. (Meredith & Black, 2006).

Therefore, more focus should be given for the development of chemical models to simulate the main combustion parameters (auto-ignition delay times, reaction progression, heat release), which are needed for the design of engines and burners, and to estimate the fuel consumption, and to model the formation of some of the main regulated pollutants (carbon monoxide, nitrogen oxides, unburned hydrocarbons and particulate matter) (Battin-Leclerc et al., 2011). “Progress in the development of chemical models has to be made together with advances in physical modeling of combustion in engines (turbulence, spray, evaporation…). What cannot be neglected is the coupling between these physical and chemical models” (Battin-Leclerc et al., 2011).

Slow progress in development of efficient preliminary design approach, optimization of practical combustion systems and study of combustion in Nepal can be linked to scarce availability of proper methodology, references and relatively easier combustion models along with complexities in computation of combustion problems. Thus, a proper mathematical model considering detailed chemical kinetics for air-fuel mixture's combustion and presentation of methodology consisting the model’s use in preliminary design of combustion systems is a must.

1.3 Objectives

1.3.1 Main objective

The main objective of the project is to carry out mathematical modeling of simple reactive systems and to perform analysis of combustion test cases.

1.3.2 Specific objectives

- To develop a mathematical model for single step and multi-step elementary chemical kinetics for various fuels.
- To extend chemical kinetics model for closed homogenous constant pressure reactor and one-dimensional flow reactor.
- To analyze combustion test cases.

1.4 Methodology

1.4.1 Literature review

Any research activity requires detailed study of the related field, getting general overview on current trends, theories and methodology, to carry out the research activity. To do so, literature review is essential.

In the first phase of the literature review, fundamental theories and concepts regarding combustion physics, combustion chemistry, chemical kinetics and flames formation and propagation were studied and gathered. Several books and research papers were studied thoroughly to gain an insight on the chemical kinetics and combustion researches. Also, the relevant data, information and descriptions were gathered from literatures, books, proceedings and online sources. Further information about selection and analysis of the combustion test cases were also obtained through books and available literatures.

The second phase deals with gathering information and data for verification of the mathematical model, consulting several books and research papers, online sources, etc.

1.4.2 Mathematical modeling

1.4.2.1 Chemical kinetics model

Mathematical modelling and generation of computer code in MATLAB for single-step and multiple elementary reactions was done. Output of chemical kinetics are directly

coupled with the reactor models so they were finally used in development of other models.

Expected Output:

- Reaction Progression
- Rate of formation and consumption of chemical species

1.4.2.2 Reactor models

The thermodynamic and flow characteristics of the system are only described, after coupling the chemical kinetics model with fundamental conservation principles. For this, following reactor models were considered.

- Closed Homogenous Constant Pressure Reactor (CHCPR)
- Premixed Non-Adiabatic Flow Reactor (PRFM)

1.4.3 Analysis of data and model verification

Chemical kinetics model was verified after analyzing results with CHEMKIN outputs for different fuels, both for single step and multiple step reactions.

For verification of developed reactor models, homogeneous constant pressure reactor and plug flow reactor in CHEMKIN were chosen and the results for same initial conditions were compared. The developed models were debugged and improved number of times to match the solutions from the developed model and CHEMKIN within desired accuracy.

After the verification of models some applications of the model in the field of combustion were analyzed.

1.4.4 Study of combustion test cases

During the preliminary design of a combustor a reference combustor was taken for required operating parameters. The developed models were used in the design of the combustor for calculating the required parameters wherever possible. For incorporating mixing and dilution ANSYS Fluent was used to finally analyze the design, and lastly the exit temperature of the combustor was checked.

Remaining test cases were studied entirely on ANSYS Fluent. The study of physics of combustion phenomenon presented in the test cases were the main objective of the study of remaining combustion test cases. So, input parameters like fuel-air ratio, velocity,

chamber dimensions, inlet temperature and pressure, etc. were varied as required to obtain desired output for temperature profile, pressure field, mass fractions of products, flame stability etc., for the test cases.

CHAPTER TWO: LITERATURE REVIEW

Knowledge of reaction mechanisms is one of the most important aspects of combustion. They define the course of a chemical reaction and determine its rate and product yield. A detailed reaction mechanism will describe not only a particular experiment carried out under specific conditions but also the entire array of available experimental data. This generality of the mechanism is valuable for prediction of course of reaction and its details under different conditions. (Basevich, 1987)

The good predictions of temperature and major species are no longer sufficient; the combustion model should also be able to predict minor species, radicals and emissions of pollutants (Alim & Malalasekera, 2009). Detailed reaction mechanisms help to establish the quantitative characteristics of combustion processes, including the rate of energy release and product yields and explanation of combustion phenomena like auto ignition, pollutants formation, etc. They are also used for optimizing and modeling combustion processes. In addition, they are useful in kinetics investigations for identifying the main reaction route and separating all secondary reactions.

Detailed reaction mechanisms can contain thousands of elementary steps among hundreds of chemical species. Main problem in construction of detailed reaction mechanisms is scarcity or lack of kinetics data on reactions which occur in combustion. The rate constant is a most important characteristic of an elementary reaction, which determines the reaction rate. Chemical reactions may deviate from actual phenomenon due to variety of uncertainties associated with the lack of necessary and reliable data on thermochemistry and reaction rate constants which affects it's the validity and accuracy (Basevich et al., 2009).

Fuels and oxidants used in combustion are large and have complex multicomponent compositions. But, mechanisms have been developed only for a limited number of simple fuel-oxidant combinations. Combustion process have enjoyed notable advance in recent years through the development of a variety of detailed chemical-kinetic mechanisms (Petrova & Williams, 2006). Many research are being conducted to gain more comprehensive and specific information about the kinetics of elementary reactions and to further improve the validity and reliability of detailed kinetics mechanisms for different fuels. (Simmie, 2003) has provided the status of development of reaction

mechanism for different hydrocarbon fuels in conjunction with the experiments that validate them.

(Hersch, 1967) analytically studied the hydrogen-oxygen chemical reaction kinetics in rocket engine combustion to calculate reaction times and concentration of chemical species during reaction for different oxygen-fuel ratios at initial temperature of 1500 to 2500 K at 20 atm. Later, (Erickson & Klick, 1970) studied the effect of the presence of small to moderate amounts of carbon dioxide (CO_2) and water vapor (H_2O) for the finite-rate constant-pressure combustion of stoichiometric hydrogen-air mixture. Computations was carried out for initial mixture temperatures of 1150 K, 1250 K, and 1500 K at a pressure of 1 atm, with additional computations for pressures of 0.5 atm and 2 atm at an initial mixture temperature of 1250 K to study the effect in induction time.

Sets of kinetic steps, or reaction mechanisms, which adequately describe the chemical processes appear to grow longer as the fuels increase in molecular weight. Each additional species adds to the computational difficulties associated with solving the differential equations in the mathematical model of the reacting system (Mclain & Rao, 1976). Generally detailed kinetic model provides much more information about combustion processes, but the use of it costs an additional CPU power (Zhukov, 2011) and often can be inconvenient to make use of the large mechanisms available. Requirement of additional computational cost and power has led to establish principal stages of combustion process for any particular conditions and obtain a reaction mechanism which is generally smaller than the detailed reaction mechanism called reduced reaction mechanism.

(Kumaran & Babu, 2009) investigated the effect of chemistry (chemical kinetics) models for combustion of hydrogen. They modeled a 3D, compressible, turbulent, reacting flow calculations with a detailed chemistry model (with 37 reactions and 9 species) and compared the results with earlier results obtained using single step chemistry. Hydrogen oxidation chemistry involves H_2, O_2, H_2O, H, O, OH, HO_2 and H_2O_2. A four-step mechanism with H_2O_2 and HO_2 assumed to be in steady state has been found to be accurate for laminar diffusion flames (Balakrishnan et al., 1995). An experimental and modelling study of methane (and ethane) oxidation at atmospheric pressure between 773 and 1573 K was carried out by (Barbe et al., 1995) in both isothermal perfectly stirred

and tubular flow reactors. They determined stable species profiles and matched these against a mechanism of 835 reactions and 42 species.

In the most common formulation, a time-dependent differential equation is written for the concentration or mole fraction of each chemical species in the system being studied. These coupled equations frequently have widely disparate characteristic time scales, referred to as ‘‘stiffness’’, and common techniques for their solution are, in general, ineffective (Westbrook et al., 2005).

Stiffness may occur for different species, in different locations, at different times or simultaneously throughout the course of an integration. Regardless of the complexity of system the equations to be solved describe species concentration which are always positive and usually tend to relax to a stable equilibrium(Oran & Boris, 1981). Classical methods for solving ordinary differential equations range from the simplest Euler method to multi-step predictor-corrector Adams-Moulton methods. They are not stable for arbitrary step sizes and thus do not handle stiff equations adequately. Packages such as VODE (Brown et al., 2006), LSODE (Hindmarsh, 1980), DASSL (Petzold, 1982) are widely adopted. Apart from these, many ODE solvers are being developed continuously to increase effectiveness and reduce cost and time of computation. MATLAB ode suite (Shampine & Reichelt, 1997) also consists stiff solvers ode15s and ode23s.

(Gordon & McBride, 1971) developed a computer program for calculation of complex chemical equilibrium compositions rocket performance incident and reflected shocks, and Chapman-Jouguet detonations. A general chemical kinetics computer program for complex, homogeneous ideal gas reactions for reaction behind a shock wave, ignition and combustion reactions in static and flowing system, combustion and nozzle expansion and general reaction in a static system or one dimensional frictional flow was done by (Bittker & Scullin, 1972). Implicit numerical integration method with variable step size procedure was used for solution of differential equations for efficient solution under wide range of conditions.

CHEMEQ (Young, 1980), LSENS (Radhakrishnan, 1994), CHEMEQ2 (Mott & Oran, 2001) and CHEMKED (Jelezniak et al., 2008) are also some programs developed for solving the stiff ordinary differential equations associated with reactive flow problems. These programs were based of solving stiff equations with numerical solvers.

CHEMKIN (R J Kee et al., 1996, 1989) is a software package whose purpose is to facilitate the formation, solution, and interpretation of problems. The package consists an Interpreter, reads a symbolic description of an elementary and Gas-Phase Subroutine Library, modular FORTRAN subroutines that may be called to return information on equation of state, thermodynamic properties, and chemical production rates involving elementary gas-phase chemical kinetics. It provides a flexible and powerful tool for incorporating complex chemical kinetics into simulations of fluid dynamics.

Cantera (Goodwin et al., 2016) is a suite of object-oriented software tools for problems involving chemical kinetics, thermodynamics, and/or transport processes. It provides types (or classes) of objects representing time-dependent reactor networks and steady one-dimensional reacting flows and is used for applications including combustion, detonations, etc.

Larger fuel molecules have large number of species and reactions and exhibit high levels of mathematical stiffness in differential equations. So, to integrate the stiff equations governing chemical kinetics, reactive flow simulations rely on implicit algorithms that require frequent Jacobian matrix evaluations. For this, numerical finite difference approximates are used but for larger chemical kinetics models this poses significant computational demands since the number of chemical source term evaluations scales with the square of species count. So, analytical Jacobian generator for chemical kinetics for accurate simulations of combustion phenomena are used in some programs like TChem (Safta et al., 2011) and pyJac (Niemeyer et al., 2017).

When early commercial CFD packages became available, simulating the complex physics inside combustion chambers was already one of the target applications. With increasing maturity of CFD technique and computing power, detailed chemical kinetics can be incorporated in design of combustion systems. Common CFD relies on solving conservation or transport equations for mass, momentum, energy of participating species. If the flow is turbulent, model equations for specific turbulent quantities have to be solved in addition.

(Hajitaheri, 2012) considers the study of new design parameters like air/fuel ratio, inlet air temperature, number of injector holes, wall temperature distribution, amount and the location of the secondary inlet air, fuel staging, fuel flow rate, and heat flux as potential variables for improvements to the combustors. So, the design of combustion systems can

be optimized from the understanding of general test cases which are used as reference for controlling the design parameters.

2.1 Mixture Properties and Chemical Kinetics

Thermodynamics determine the equilibrium state of chemically reactive system. It can easily describe the system for fast chemical reactions. But, in most of the cases, chemical reaction occurs on comparable time scales. So, information about the rate of chemical reaction is required which is given by chemical kinetics.

The mole fraction of the species i, $X_{i,}$ is defined as the fraction of the total number of the moles in the system that are species i. i.e.

$$X_i = \frac{N_i}{N_1 + N_2 + \cdots N_i + \cdots} = \frac{N_i}{N_{tot}} \tag{2-1}$$

Similarly, the mass fraction of the species i, Y_i, is the amount of mass of species i compared with the total mixture mass:

$$Y_i = \frac{m_i}{m_1 + m_2 + \cdots m_i + \cdots} = \frac{m_i}{m_{tot}} \tag{2-2}$$

The equation of state is

$$P = \frac{\rho RT}{MW_{mix}} \tag{2-3}$$

Mole fraction and mass fractions are readily converted from one to another using the molecular weights of the species of interest and of the mixture:

$$Y_i = X_i \frac{MW_i}{MW_{mix}} \tag{2-4}$$

$$X_i = Y_i \frac{MW_{mix}}{MW_i} \tag{2-5}$$

The mixture molecular weight MW_{mix}, is easily calculated from the knowledge of either the species mass or mole fraction:

$$MW_{mix} = \sum_i X_i \, MW_i \tag{2-6}$$

$$MW_{mix} = \frac{1}{\sum_i Y_i \, MW_i} \tag{2-7}$$

Molar concentration can be calculated from mole fraction:

$$[X_i] = X_i \frac{P}{R\Sigma X_i T_i} \tag{2-8}$$

Mean mass density is defined by

$$\rho = \sum_{i=1}^{N_{sp}} [X_i]\, MW_i \tag{2-9}$$

The equivalence ratio ϕ is the ratio of actual fuel-air mixture to that required for stoichiometric fuel-air mixture.

$$\phi = \frac{\left(\frac{Fuel}{Air}\right)_{actual}}{\left(\frac{Fuel}{Air}\right)_{stoic}} \tag{2-10}$$

2.2 Premixed Reactors

To couple the chemical kinetics with thermodynamic and flow characteristics of air fuel mixture, a reactor model is required. A reactor model is the one made by coupling chemical kinetics, which gives generation terms, with the fundamental conservation equations of the physical properties.

2.2.1 Closed Homogenous Constant Pressure Reactor Model

Closed homogenous constant pressure reactor is like a system of reactants confined in a piston-cylinder arrangement that react at each and every location within the gas volume at the same rate. Thus, there are no temperature or composition gradients within the mixture, and a single temperature and set of species concentrations suffice to describe the evolution of the system. For exothermic combustion reactions, both the temperature and volume will increase with time, pressure held constant.

2.2.2 Premixed Reactive Flow Model

General combustion devices are long and slender, as in a gas-turbine combustion chamber, a cement kiln or a gasifier, in which air fuel mixture enter at one end and products leave at the other. Such devices can be idealized as plug-flow thermochemical reactors. In this reactor operating in steady state, properties such as velocity, temperature, pressure, and mass fractions of species vary principally along the length of the reactor

(Date, 2011). Therefore, for such reactors, equations of mass, momentum, and energy can be simplified to their one-dimensional forms.

2.3 Combustion modelling and study of Test Cases

Development and optimization of combustion systems require deep understanding of the physics of combustion. Various parameters like the adiabatic flame temperature, flow velocity, mixing of fuel and air dictate the performance of the combustion system. So, numerous combustion test cases for flame holding, mixing and mainly decreasing the length of the combustion chamber and controlling temperature in combustors are studied widely.

Holding of the flame within required length of combustion chamber is required in major design of premixed combustion systems. Thus, test cases for completing combustion within desired length of the combustor and its effect on various other parameters like temperature profile, species concentration distribution can be studied. Variation of concentration of fuel in reactants and reactants inlet velocity also can be studied for temperature distribution profiles and other combustion phenomenon in the chambers.

For non-premixed reactive flows; mixing enhancing techniques are mostly important in design. Flame height and radius of flame in co flow is determined by mass diffusion and volume flow rate which should be known prior to manufacturing of the combustor. Proper combustion in non-premixed flows is directly dependent on the mixing of fuel and oxidizer. Thus, various orientations of injection of fuel and air in the combustion chamber can be studied in case of non-premixed combustion systems for improving mixing and thus improving reaction rate.

Test Cases

- Preliminary design of Gas Combustor
- Premixed Flow Combustion
- Cavity Stabilized Combustion
- Bluff Body Stabilized Combustion

CHAPTER THREE: MATHEMATICAL MODELS

Mathematical modelling and solver development in MATLAB is discussed in this chapter.

3.1 Chemical Kinetics Model

For an elementary reaction involving N_{sp} chemical species that can written in form

$$\sum_{i=1}^{N_{sp}} \nu'_{ki}\chi_i \leftrightharpoons \sum_{i=1}^{N_{sp}} \nu''_{ki}\chi_i \tag{3-1}$$

where ν'_{ki} and ν''_{ki} are stoichiometric coefficients on reactants and products side for i^{th} species in k^{th} reaction and χ_i is chemical symbol for i^{th} species.

3.1.1 Species Production Rate

The rate of production of species ω_i is given by

$$\dot{\omega}_\iota = \sum_{k=1}^{N_{rec}} \nu_{ki} q_k \tag{3-2}$$

where ν_{ki} is overall stoichiometric coefficient for species i in reaction k, q_k rate of progress variable/production and N_{rec} is number of reactions. Also,

$$\nu_{ki} = \nu''_{ki} - \nu'_{ki} \tag{3-3}$$

where ν''_{ki} and ν'_{ki} are the product and reactant stoichiometric coefficients respectively of species i in reaction k and

$$q_k = c_k \left(k_{f,k} \prod_{j=1}^{N_{sp}} [X_j]^{\nu'_{jk}} - k_{r,k} \prod_{j=1}^{N_{sp}} [X_j]^{\nu''_{jk}} \right) \tag{3-4}$$

where $k_{f,k}$ and $k_{r,k}$ are the forward and reverse reaction rate coefficients for k^{th} reaction respectively and c_k is third body modification and is given by

$$c_k = \begin{cases} 1 \text{ for elementary reactions} \\ [M] \text{ for third} - \text{body enhanced reactions} \end{cases} \tag{3-5}$$

For the presence of third body, the reaction is modified by the third body concentration $[M]$ by

$$[M] = \sum_{i=1}^{N_{sp}} \alpha_{ki} [X_i] \tag{3-6}$$

where α_{ki} is the third body efficiency of i^{th} species in k^{th} reaction and the rate of production q_k becomes:

$$q_k = \sum_{i=1}^{N_{sp}} \alpha_{ki} [X_i] \left(k_{f,k} \prod_{j=1}^{N_{sp}} [X_j]^{\nu'_{jk}} - k_{r,k} \prod_{j=1}^{N_{sp}} [X_j]^{\nu''_{jk}} \right) \tag{3-7}$$

All the species of mixture can contribute equally as third body or a single species may act as the third body.

3.1.2 Forward Rate Coefficient

The forward reaction rate coefficient $k_{f,k}$ are generally assumed to follow Arrhenius temperature dependence and is given by

$$k_{f,k} = A_{r,k} T^{n_k} \exp\left(\frac{-E_{a,k}}{RT}\right) \tag{3-8}$$

where $A_{r,k}$= pre-exponential factor, n_k =temperature exponent, $E_{a,k}$= activation energy, R = gas constant and T = temperature.

3.1.3 Reverse Rate Coefficient

Irreversible reactions have zero reverse rate coefficient $k_{r,k}$ while reversible reactions have nonzero $k_{r,k}$. For reversible reactions, $k_{r,k}$ is determined in one of the two ways:

a. Explicit reverse Arrhenius parameters exactly like $k_{f,k}$.
b. Ratio of the forward rate coefficient $k_{f,k}$ and the equilibrium constant $K_{C,k}$

$$k_{r,k} = \frac{k_{f,k}}{K_{C,k}} \tag{3-9}$$

3.1.4 Chemical Equilibrium

The equilibrium constant for concentration is calculated by

$$K_{c,k} = K_{P,k} \left(\frac{P_{atm}}{R_u T}\right)^{\sum_{k=1}^{N_{sp}} \nu_{ki}}$$

where P_{atm} is pressure of one standard atmosphere in atm and R_u is universal gas constant in cm^3- atm-K^{-1}-$mol^{-1}$and $K_{P,k}$ is equilibrium constant and calculated by

$$K_{P,k} = \exp\left(\frac{-[\Delta H_k^o - T\Delta S_k^o]}{RT}\right) = exp\left[\sum_{i=1}^{N_{sp}} \nu_{ki}\left\{\frac{-(H_i^o - TS_i^o)}{RT}\right\}\right] \quad (3\text{-}10)$$

where H_i^o and S_i^o are standard state enthalpy and entropy at one atmosphere and calculated from following equations used by (Gordon & McBride, 1971).

$$\frac{H_i^o}{R} = a_{1i}T_i + \frac{a_{2i}}{2}T_i^2 + + \frac{a_{3i}}{3}T_i^3 + \frac{a_{4i}}{4}T_i^4 + \frac{a_{5i}}{5}T_i^5 + a_{6i} \quad (3\text{-}11)$$

$$\frac{S_i^o}{R} = a_{1i}lnT_i + a_{2i}T_i + \frac{a_{3i}}{2}T_i^2 + \frac{a_{4i}}{3}T_i^3 + \frac{a_{5i}}{4}T_i^4 + a_{7i} \quad (3\text{-}12)$$

Similarly,

$$\frac{C_{p,i}^o}{R} = a_{1i} + a_{2i}T_i + a_{3i}T_i^2 + a_{4i}T_i^3 + a_{5i}T_i^4 \quad (3\text{-}13)$$

Units are in molar units.

The mass based specific heat and enthalpy are then calculated by

$$c_{p,i}^o = \frac{C_{p,i}^o}{M_i} \quad (3\text{-}14)$$

$$h_{p,i}^o = \frac{H_{p,i}^o}{M_i} \quad (3\text{-}15)$$

3.2 Closed Homogenous Constant Pressure Reactor (CHCPR)

In CHCPR, the system's mass is constant with no inflow and outflow of species from the system. The thermodynamic properties are uniform and homogenous only varying with time. The system is transient zero-dimensional with rate of conversion of reactants to products is controlled by chemical reaction rates only. The conservation equations; mass conservation, species conservation, energy conservation and equation of state, are used to derive the equations for closed homogenous constant pressure reactor with assumptions:

- Some reaction rate depends on pressure as well as temperature but only temperature dependence is considered in solver.
- No phase change during reaction.

- No surface reactions
- No heat transfers between the surface and surrounding

Since the system is zero dimensional, the effects of fuel injection and mixing cannot be included. However, it can predict ignition and reaction and also provide a lower limit of times required for reaction.

3.2.1 Governing Equations

The system of conservation equations and chemical reactions form a coupled set of ordinary differential equations. The final set of equations obtained are:

$$\frac{dT}{dt} = \frac{\sum_i (H_i \dot{\omega}_\iota)}{\sum_i ([X_i] C_{p,i})} \tag{3-16}$$

$$\frac{d[X_i]}{dt} = \dot{\omega}_\iota - [X_i] \left[\frac{\sum \dot{\omega}_\iota}{\sum_j [X_j]} + \frac{1}{T} \frac{dT}{dt} \right] \tag{3-17}$$

3.2.2 Rate of Heat Production

The products of a chemical reaction are not only new chemical compounds, but releasing or consuming of heat as well due to difference in energies between products and reactants. For constant pressure process, the rate of heat production is given by

$$q_v = \sum_{i=1}^{N_{sp}} \dot{\omega}_\iota H_i \tag{3-18}$$

where $\dot{\omega}_\iota$ is given by (3-2) and H_i is given by (3-11) and must be in molar units. Then, value of q_v is in J/cm^3-sec.

3.3 Premixed Reactive Flow Model (PRFM)

Control volume approach is used to describe a premixed reactive flow. In this approach physical properties' outflow and inflow is balanced with rate of generation and temporal change of the property in a control volume system. Using a general variable as the physical property per unit mass (φ), the conservative form of the property for a control volume can usefully be written in the following form:

$$\frac{\partial \rho \emptyset}{\partial t} + \nabla(\rho \emptyset . \boldsymbol{V}) = \nabla(\Gamma \nabla \emptyset) + S_\emptyset \tag{3-19}$$

In the context of reactive flow, mixture mass conservation, species mass conservation, momentum conservation and energy conservation will be taken into account along with ideal gas equation. Heat flow in and out of the reactor is modelled adding heat flux source term in energy equation. Injection of any species or combination of species through any portion of lateral surface of the reactor is incorporated as an additional source term in RHS of conservation of mixture mass, species mass, momentum and energy.

The assumptions made for the reactor model are:

- Steady state.
- Fuel and air is premixed. The input mixture of fuel and air is fully mixed.
- Uniform properties in the direction of flow i.e. one dimensional flow. That means the variation of velocity, temperature, pressure etc. in the direction perpendicular to the flow is assumed negligible.
- Species transport due to thermal and mass diffusivities are neglected due to domination of advective transport in the only one properties varying dimension.
- Ideal frictionless flow with ideal gas behavior.
- The rate of conversion of reactants to products is controlled by chemical reaction rates only. Mixing process does not affect the conversion.
- No surface reactions.

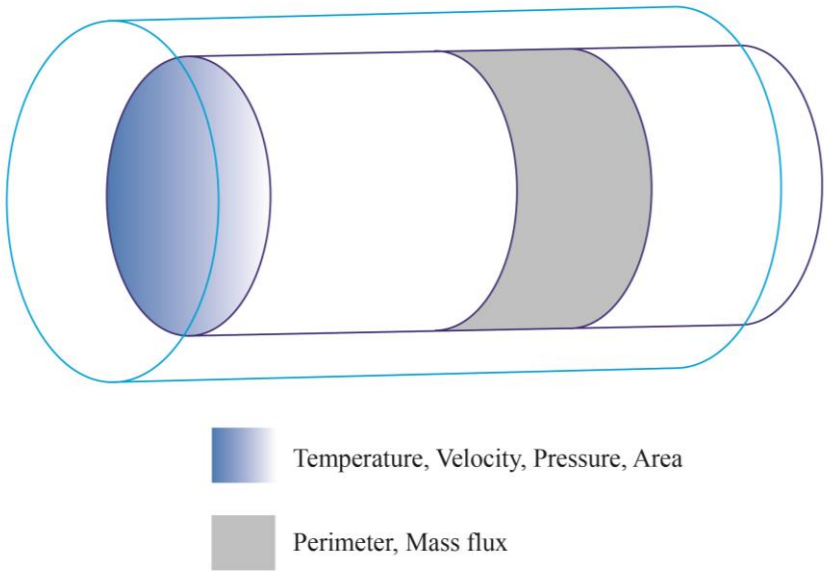

Figure 3-1 PRFM illustration

The conservation equations that will be used in the premixed reactive flow model are

- Conservation of mixture mass:

$$\frac{\partial(\rho u A)}{\partial x} = \dot{m}_L{}'' \mathcal{P} \tag{3-20}$$

- Conservation of mass of the i[th] species:

$$\frac{\partial(Y_i)}{\partial x} = \frac{\dot{\omega}_\iota}{\rho u} MW_i + \frac{Y_{i_L} \dot{m}_L{}'' \mathcal{P}}{\rho u A} \quad \text{for i} = 1,2,\dots,\text{N.} \tag{3-21}$$

- Conservation of x-momentum:

$$\frac{\rho u \partial(u)}{\partial x} = -\frac{\partial p}{\partial x} + \frac{\dot{m}_L{}'' u \mathcal{P}}{A} \tag{3-22}$$

- Energy conservation equation:

$$\frac{c_p \partial T}{\partial x} + u\frac{\partial(u)}{\partial x} = -\Sigma h_i \frac{\partial(Y_i)}{\partial x} + \frac{(\dot{m}_L{}'' h_L - \dot{\mathrm{Q}}'')\mathcal{P}}{\rho u A} \tag{3-23}$$

- Residence time:

$$\frac{dtr}{dx} = \frac{1}{u} \tag{3-24}$$

where,

u	Velocity in x-direction
ρ	Mass density
p	Pressure
$\dot{\mathrm{Q}}''$	Heat flux outflow from reactor wall
$\mathcal{P}$	Perimeter of the reactor
A	Cross-section area of the reactor
h_L	Total specific enthalpy of injected mass
$\dot{m}_L$	Injected mass flux defined at specific discrete grid points
Y_{i_L}	Mass fraction of injected mass defined at specific discrete grid points

Equations (3-20), (3-22) and (3-23) along with ideal gas equation are coupled into two equations by eliminating some derivatives by substitution and the set of obtained equations are:

$$\frac{d\rho}{dx} = \frac{\frac{\rho P}{c_p T}\left[\frac{u^2 \dot{m}_L{}'' \mathcal{P}}{\rho u A} + \sum_i \left\{\frac{d(Y_i)}{dx}\left(h_i - \frac{MW_{mix}}{MW_i} c_p T\right)\right\} - \frac{(\dot{m}_L{}'' h_L - \dot{Q}'')}{\rho u A}\mathcal{P}\right]}{p\left(1 + \frac{u^2}{c_p T}\right) - \rho u^2} \quad (3\text{-}25)$$

$$\frac{dT}{dx} = \frac{1}{c_p}\left(\frac{u^2}{\rho}\frac{d\rho}{dx} - \frac{u^2 \dot{m}_L{}'' \mathcal{P}}{\rho u A} - \sum_i h_i \frac{d(Y_i)}{dx} + \frac{(\dot{m}_L{}'' h_L - \dot{Q}'')}{\rho u A}\mathcal{P}\right) \quad (3\text{-}26)$$

3.4 Solver

The developed solver are not just programs that are designed to accept input, solve a problem and give the output. It is a tool intended to help user to work efficiently and effectively with large number of chemical reactions.

3.4.1 Inputs

3.4.1.1 Chemical Reaction Mechanism

It is the input file to the interpreter. It consists of reactions involved along with pre-exponential factor $A_{r,k}$, temperature exponent n_k and activation energy $E_{a,k}$. It also consists of the elements and species involved in the chemical reactions. The global reaction with composition of fuel and oxidizers should be present if one of the inputs is equivalence ratio (ϕ). The format for the chemical input file is as in Appendix A. "%%" indicates start of comment statement.

3.4.1.2 State Variables

Interpreter extracts all the required information about the elements, species and reactions involved in chemical reaction as defined by reaction mechanism. Apart from that, some state parameters at initial conditions (t=0, x=0) are required for proper defining of state of reacting mixture.

- Pressure or density
- Temperature

- Species Mole Fraction, Species Mass Fraction, Species Concentration or Equivalence Ratio

Once state parameter, one from each point, is defined equation (2-1) to (2-10) can be used to obtain the others. If equivalence ratio is one of the inputs, global reaction, fuel composition and oxidizer composition should be provided in chemical reaction mechanism file.

3.4.2 Preprocessor

The preprocessor package consists of:

1. Thermodynamic Database (file)
2. Atomic Mass Database (file)
3. Interpreter (code)

3.4.2.1 Thermochemical Data File 'thermo.dat'

Thermochemical data file Appendix B consists of species name, elemental composition of species i.e. no of elements in each species, three temperatures for defining two temperature range and seven curve fitting data coefficients for standard state enthalpy, specific heat and entropy with for each specified temperature range. The thermodynamic information has same format as that used by (Gordon & McBride, 1971)**.** The solver thermodynamic database is the extract of the database (Burcat & Branko, 2005).

3.4.2.2 Atomic Mass Database

Atomic mass of each element in modern periodic table and some isotopes is contained in 'mass_table.txt' file

3.4.2.3 Interpreter

The interpreter first processes the chemical reaction mechanism file and then extracts the required thermochemical data for each species in reaction file. Furthermore, it also extracts, the atomic mass of the elements on reaction file and calculates the atomic weight of each species. i.e. interpreter extracts all the required information about the elements, species and reactions involved in chemical reaction as defined by reaction mechanism.

Interpreter checks the elemental conservation for product and reactant side. If conservation is satisfied stoichiometric values are the assigned values. If not satisfied, it balances the reaction using the method developed by (Blakley, 1982).

For reaction: $CH_4+O_2=CO_2+H_2O$

It is written in matrix form as A= $\begin{bmatrix} CH_4 & O_2 & CO_2 & H_2O & \\ 4 & 0 & 0 & 2 & H \\ 1 & 0 & 1 & 0 & C \\ 0 & 2 & 2 & 1 & O \end{bmatrix}$

X=$\begin{bmatrix} CH_4 \\ O_2 \\ CO_2 \\ H_2O \end{bmatrix}$

Then Gauss-Jordan Elimination by row reduction is used to above matrix to obtain

$$A=\begin{bmatrix} 1 & 0 & 0 & 0.5 \\ 0 & 1 & 0 & 1 \\ 0 & 0 & 1 & -0.5 \end{bmatrix}$$

Finally, Linear algebra AX=0 is used to obtain the value of X. The values of X is extracted such that they are the smallest integer possible.

$$X=\begin{bmatrix} -1 \\ -2 \\ 1 \\ 2 \end{bmatrix}$$

Interpreter outputs:

- Number of species, no. of elements in each species, balanced chemical reactions, pre-exponential factors, activation energies of each reactions
- Temperature dependent thermodynamic properties of species like molar heat capacities, molar enthalpies, molar entropies for temperature ranging from 300-5000 K.

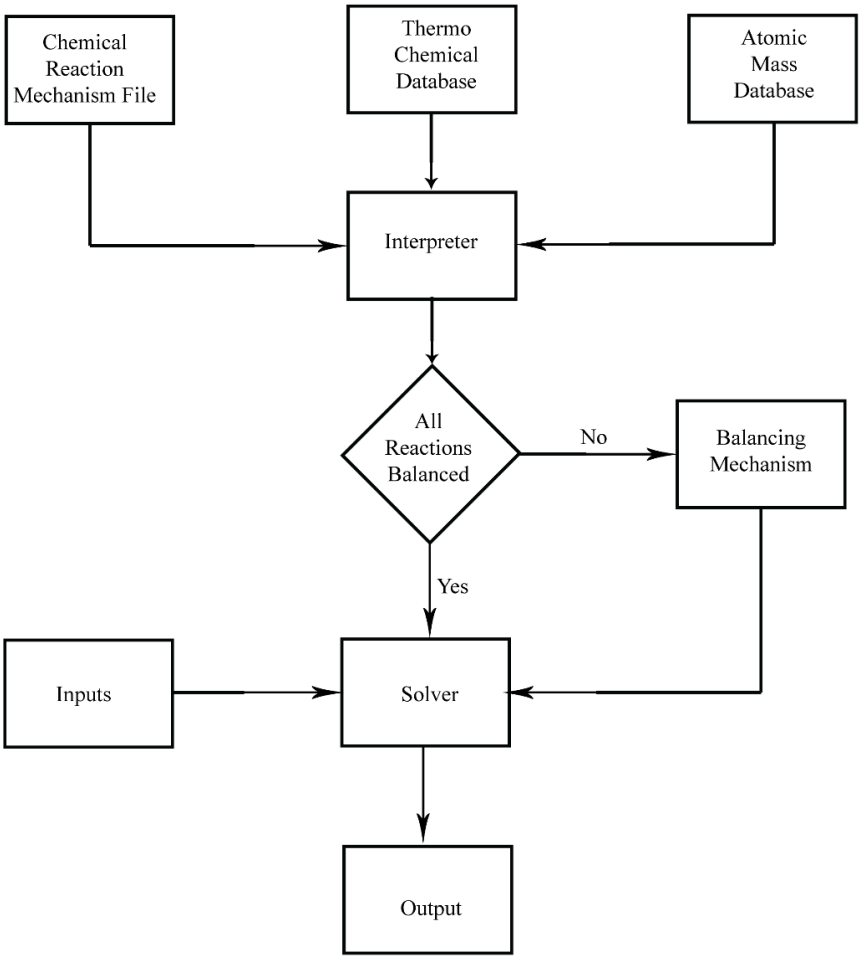

Figure 3-2 Interpreter-Solver Chart

3.4.3 MATLAB Solvers

Main solver consists of three solvers:

- Chemical Kinetics Solver
- Constant Closed Homogenous Constant Pressure Solver
- Premixed Reactive Flow Solver

3.4.3.1 Chemical Kinetics Solver

It solves equation from (3-2) - (3-15) to obtain production rate $\dot{\omega}_\iota$.

The inputs required for the kinetics solver are:

- Chemical Reaction Mechanism
- State Variables

Outputs obtained are:

- Rate of production of every species (ω_i)

3.4.3.2 Closed Homogenous Constant Pressure Reactor Solver

CHCPR equations (3-16) and (3-17) are stiff non-linear ordinary differential equations. Thus, they constitute initial value problem with total number of unknowns N_{sp}+1 represented by array y= $[T\ [X_1]\ [X_2]\ \ldots.\ [X_{N_{sp}}]]^T$

$$y' = f(x) = \begin{bmatrix} \frac{dT}{dt} \\ \frac{d[X_1]}{dt} \\ \vdots \\ \frac{d[X_{N_{sp}}]}{dt} \end{bmatrix} \tag{3-27}$$

with $T\ (t = 0) = T_0$ and $[X_i](t = 0) = [X_i]_0$

MATLAB's ode15s solver was used to solve equation (3-27) by coupling with Chemical Kinetics Solver to obtain following outputs:

- Volumetric heat generation rate
- Temperature variation with reaction progression
- Species mass and mole fractions with reaction progression

Applications of CHCPR

- Obtaining time scale of the reaction (i.e. ignition time and reaction time)
- The principal parameters of these calculations are the initial static pressure and temperature and the hydrogen-air mixture composition. These parameters can be varied to study effects on ignition, flame temperature, final composition, etc.
- Studying the effect of presence of different species in the oxidizer
- Studying the effect of equivalence ratio on the adiabatic flame temperature and final composition

Discussion

- Initial conditions

  $T\ (t = 0)$ = 1500 K

  φ = 1

  $p\ (t = 0)$ = 2.95 atm

  Fuel = H_2

  Oxidizer = 0.21 O_2 and 0.79 N_2

  Reaction Mechanism = Appendix A (Robert J Kee et al., 1996)

Reaction mechanism in Appendix A for the developed code and CHEMKIN were provided with same initial conditions as mentioned above. **(Figure 3-3)** to **(Figure 3-7)** shows molar fraction of different species, temperature, volumetric heat release, etc., progressing in time. The plot clearly shows that the results of from the developed code and CHEMKIN were equivalent. Thus, the developed code predicts the finite rate of chemical reaction as accurately as the commercial software CHEMKIN for detailed chemical reactions.

While using ode15s for large number of species in reaction mechanism, large errors were encountered. Adjusting the relative and absolute tolerances reduced some of these errors, but consistent, effective values for all the states could not be found. It required unreasonably small tolerances (below 1×10^{-25}). Despite these small tolerances, the errors encountered were large sue to large concentration disparities. Furthermore, tolerances and step size could not be decreased below certain limit due to computational limit.

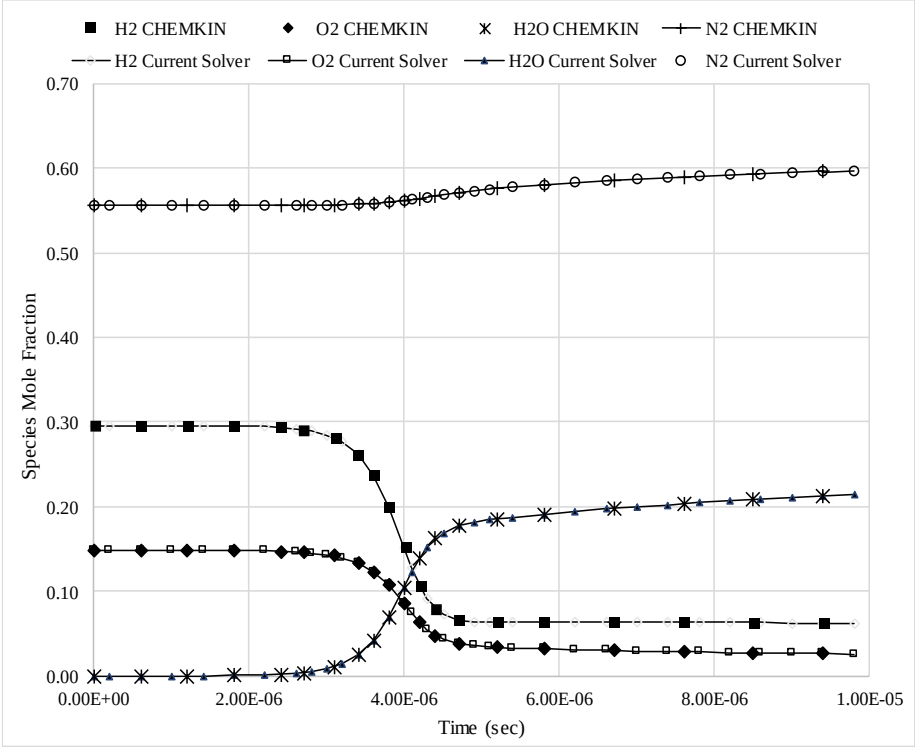

Figure 3-3 Variation of major species' mole fraction with time for ϕ=1, 1500 K, 2.95 atm hydrogen-air mixture in CHCPR compared with CHEMKIN

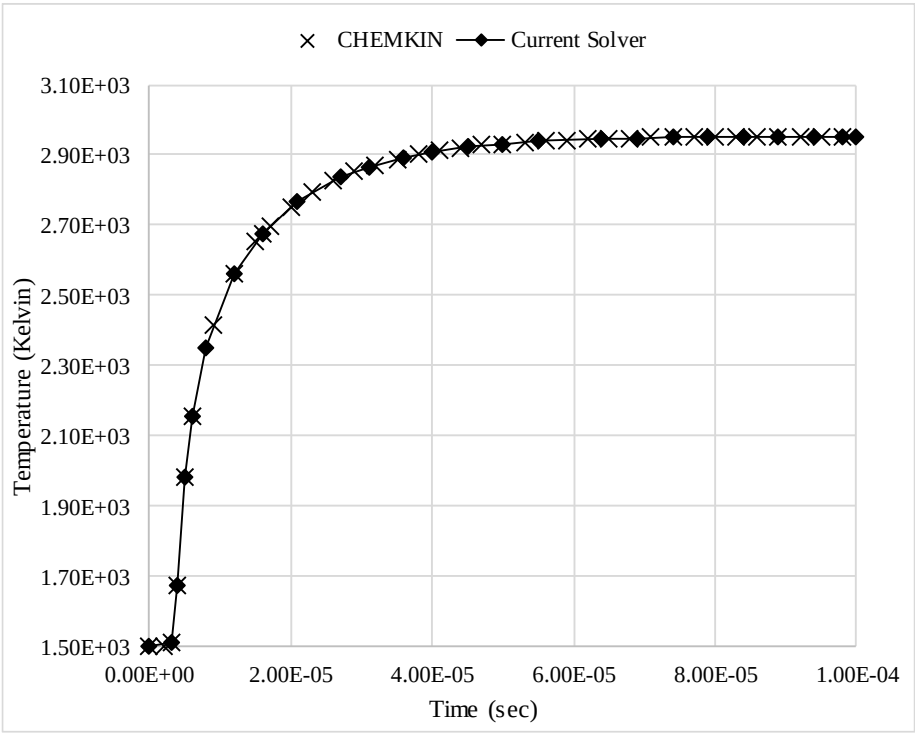

Figure 3-4 Variation of temperature with time for ϕ=1, 1500 K, 2.95 atm hydrogen-air mixture in CHCPR compared with CHEMKIN

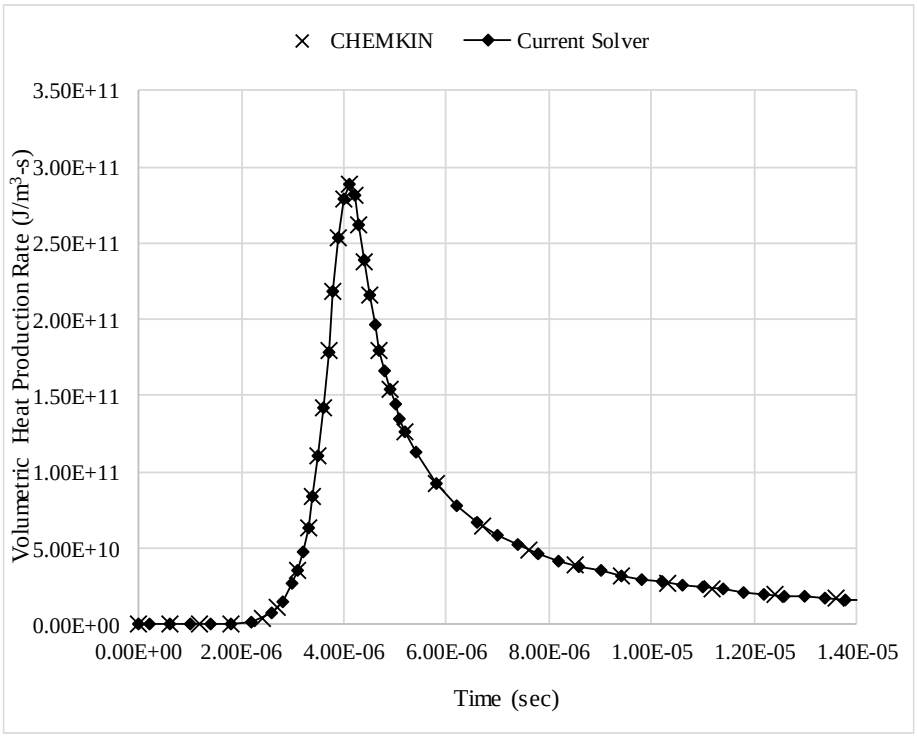

Figure 3-5 Volumetric heat production rate with time for ϕ=1, 1500 K, 2.95 atm hydrogen-air mixture in CHCPR compared with CHEMKIN

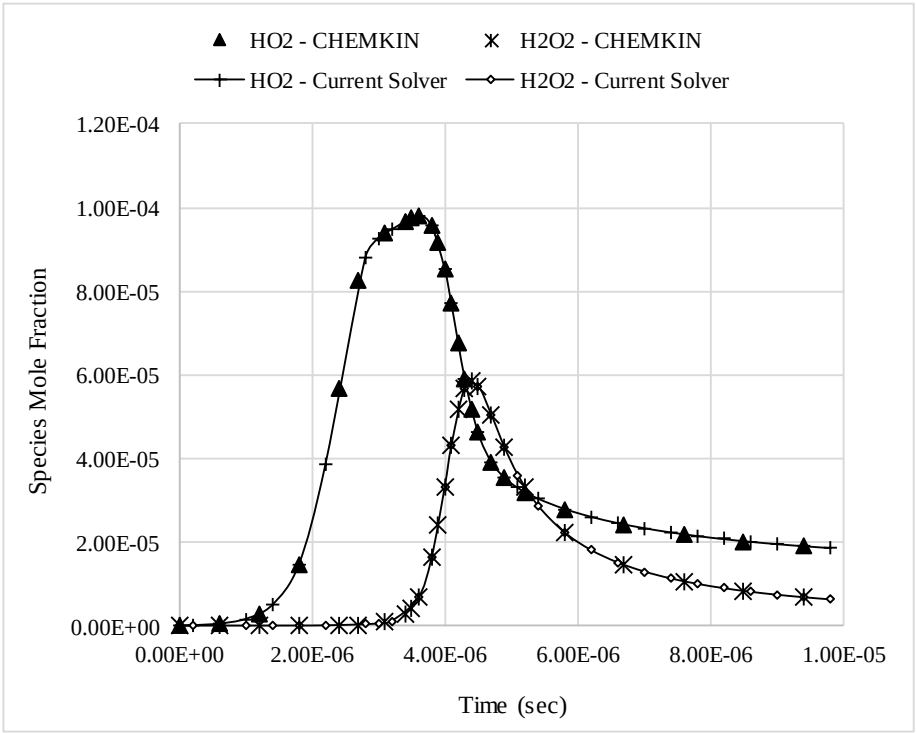

Figure 3-6 Variation of intermediate species' mole fraction with time for ϕ=1, 1500 K, 2.95 atm hydrogen-air mixture in CHCPR compared with CHEMKIN

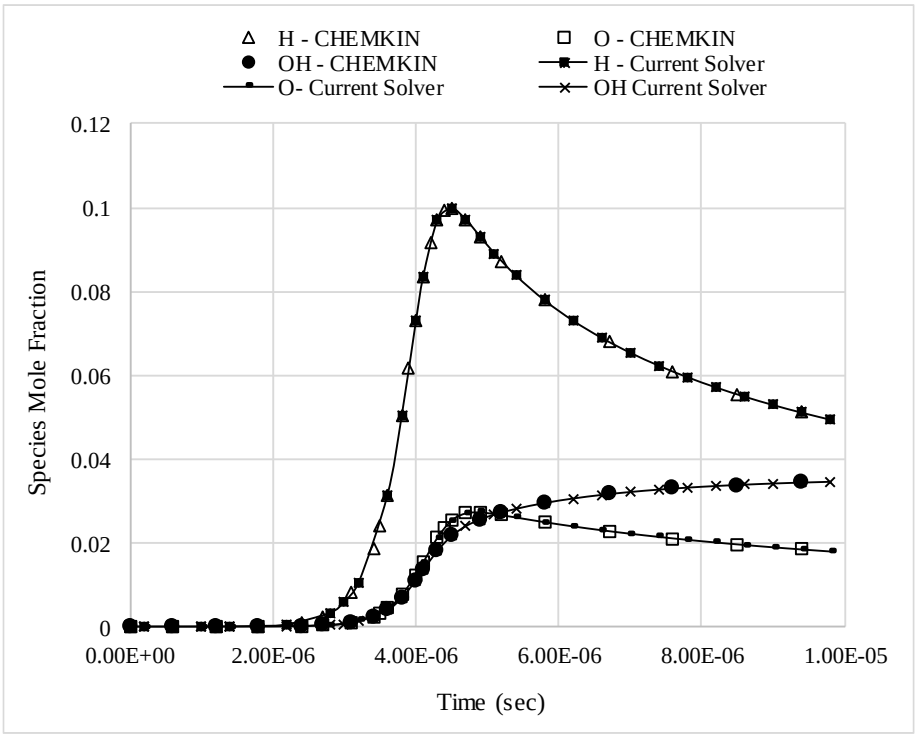

Figure 3-7 Variation of intermediate species' mole fraction with time for ϕ=1, 1500 K, 2.95 atm hydrogen-air mixture in CHCPR compared with CHEMKIN

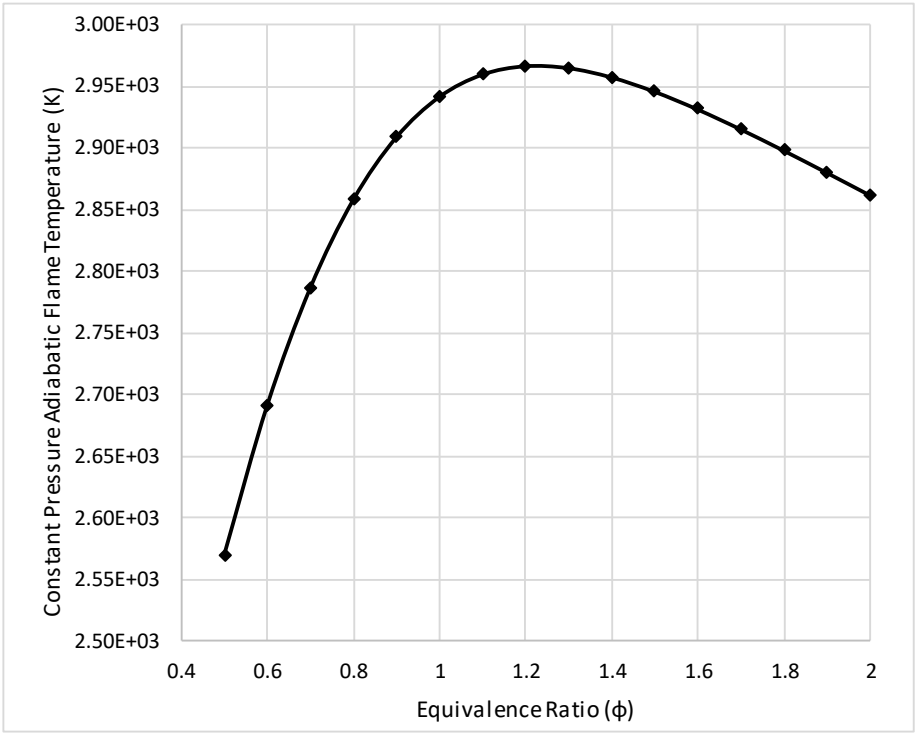

Figure 3-8 Constant Pressure Adiabatic Flame Temperature vs Equivalence ratio (ϕ) for 1500 K, 2.95 atm, hydrogen-air mixture in CHCPR

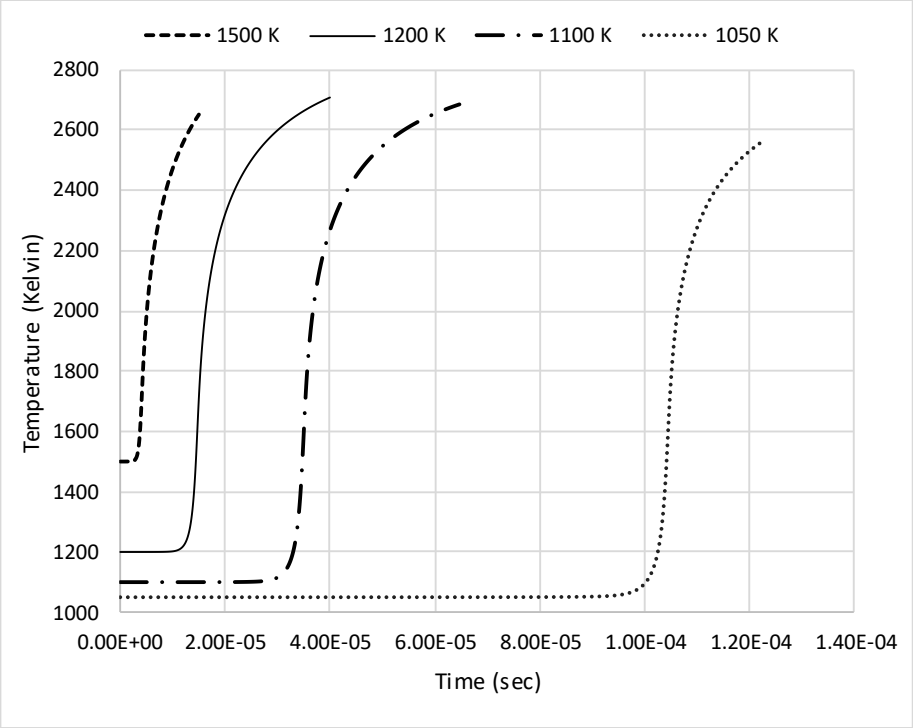

Figure 3-9 Auto-ignition delay against Initial temperature for ϕ=1, 2.95 atm hydrogen air mixture in CHCPR

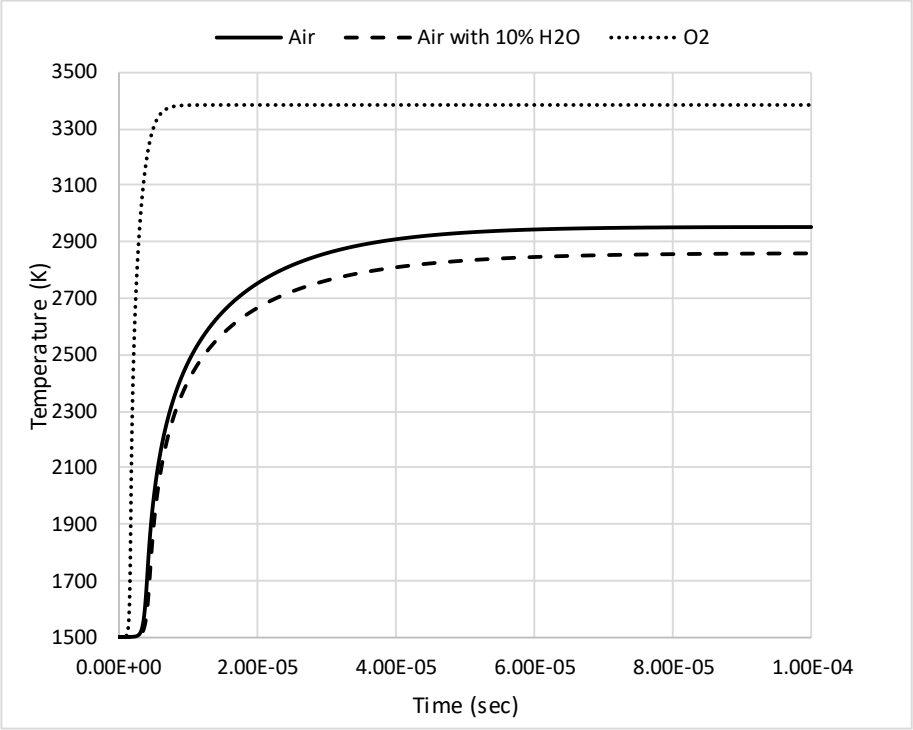

Figure 3-10 Variation of adiabatic flame temperature with oxidizer diluent for ϕ=1, 1500 K, 2.95 atm during hydrogen combustion

3.4.3.3 Premixed Reactive Flow Solver

Thus, the final set of equation are (3-21), (3-24), (3-25) and (3-26) which contains $\frac{dT}{dx}$, $\frac{d\rho}{dx}$, $\frac{dtr}{dx}$ and $\frac{d(Y_i)}{dx}$.

The equations constitute initial value problem with total number of unknowns N_{sp}+3 represented by array y = $[T\ tr\ \rho\ Y_1\ \ Y_2 \ldots . Y_{N_{sp}}\ ]^{\mathrm{T}}$.

$$y' = f(x) = \begin{bmatrix} \frac{dT}{dx} \\ \frac{dtr}{dx} \\ \frac{d\rho}{dx} \\ \frac{dY_1}{dx} \\ \vdots \\ \frac{dY_{N_{sp}}}{dx} \end{bmatrix} \tag{3-28}$$

with $T\ (x = 0) = T_0$, $Y_i(x = 0) = Y_{i_0}$, $p\ (x = 0) = p_0$ and $u\ (x = 0) = u_0$,

$tr\ (x = 0) = 0$.

The equation (3-28) was solved by Newton-Raphson method for the solution of systems of non-linear ODEs. The solution procedure is shown in **(Figure 3-11)**.

The steps involving solution of system of non-linear ODEs are:

Formulation of governing equations based on assumptions

Equations are in the form of systems of non-linear ODEs

First order backward difference approximation of ODEs

Write the equations in the form of function (F) = 0

Find approximate jacobian matrix [J]

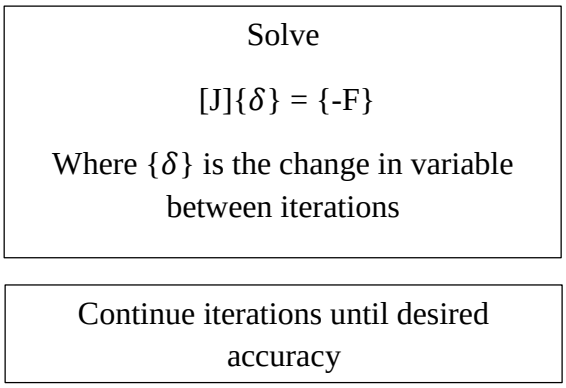

Figure 3-11 Newton-Raphson solution technique

Outputs

- Volumetric heat generation rate
- Temperature variation with length
- Density variation with length
- Velocity variation with length
- Pressure variation with length
- Species mass and mole fractions with length

Applications

- Preliminary length scale of combustion chamber
- Effect of flow on chemical reactions
- Effect of wall heat flux in the chamber/reactor results in more accurate auto ignition characteristics than CHCPR in reactive flow
- Preliminary study of combustion chamber, incorporating number of zones of combustion in the combustor as the code also includes injection of flue along the length

Discussion

The present solver of PRFM was compared with CHEMKIN gas phase plug flow reactor and Cantera (Goodwin et al., 2016) provided one-dimensional freely propagating flame solution using reduced version of UCSD mechanism involving 9 species and 21 reactions (UCSD, 2014). The initial conditions being:

Initial Temperature	:	1215.418 K
Initial Velocity	:	8.711493 m/sec
Initial Pressure	:	100000 Pa

Table 3-1 Initial mole fraction used for PRFM verification

H_2	0.125843
H	0.026189
O_2	0.095631
O	0.004663
OH	0.002996
HO_2	7.80146e-05
H_2O_2	9.91e-06
H_2O	0.137043
N_2	0.607547

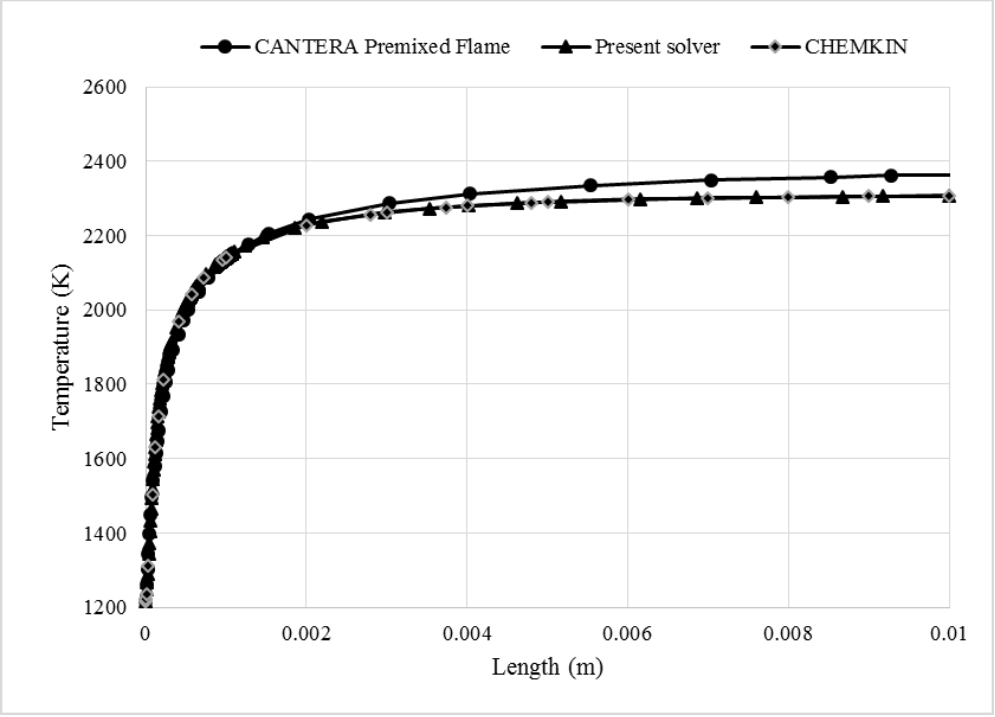

Figure 3-12 Variation of temperature with length for 1215.418 K, 1 bar, 8.711493 m/sec, Table 3-1 mixture in PRFM compared with CHEMKIN and Cantera Premixed Flame

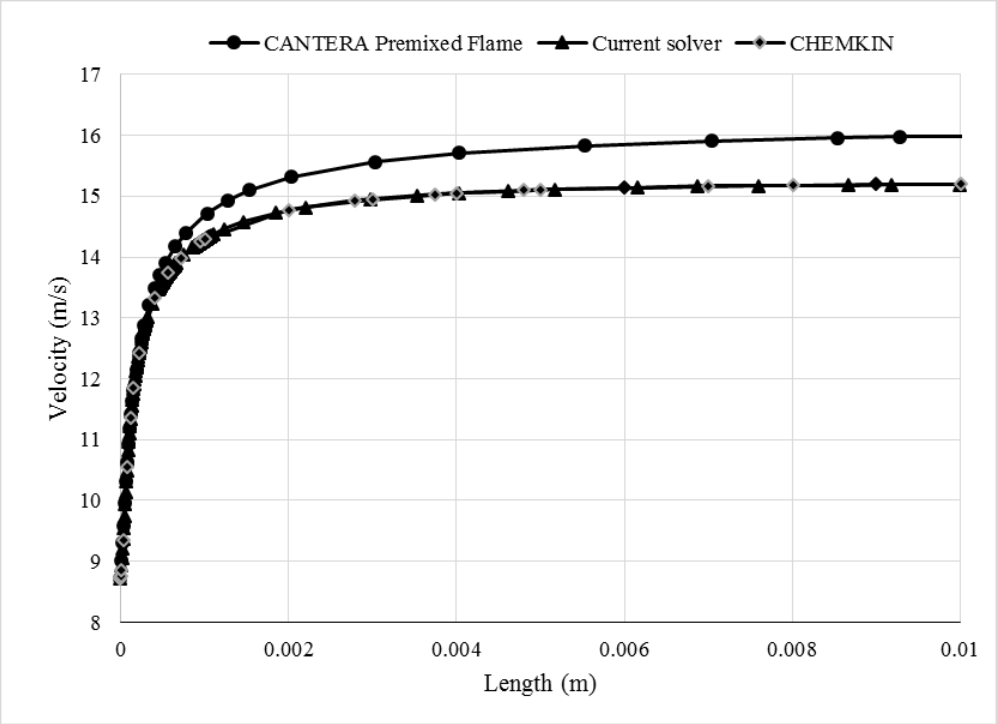

Figure 3-13 Variation of velocity with length for 1215.418 K, 1 bar, 8.711493 m/sec, Table 3-1 mixture in PRFM compared with CHEMKIN and Cantera Premixed Flame

Present solver and CHEMKIN results match with significant accuracy whereas Cantera Premixed Flame results does not. The reason may be that inputs like all the assumptions, thermochemical data, reaction enhancements, etc. for present code and CHEMKIN results are exactly the same whereas it cannot be assured for Cantera results.

When initial temperature was below 1100 K or large number of reacting species were present, it caused to large disparities in the species concentration. Due to this, it caused problem in selecting appropriate step size for reaction progression. The step size under some conditions had to be decreased below 10^{-12} which increased the computational time drastically.

CHAPTER FOUR: COMBUSTION TEST CASES

4.1 Gas Combustor Test Case

A simple gas combustor test case was equipped using the collective results of both CHCPR and PRFM. The non-premixed and turbulent mixing considerations of the test case was further carried out in ANSYS Fluent.

Since the CHCPR and PRFM are both bound to premixed laminar finite rate reaction. The effect of turbulent non-premixed property of gases cannot be accounted using the models. A gas combustor is a long and slender tube in which air fuel mixture enter at one end and products leave at the other. The fuel is injected at the inlet of the chamber which gets mixed with high velocity turbulent air entering the tube. The localized premixed zones in the combustor reacts on external ignition to form products and energy. The ignition provides enough activation energy and temperature to trigger reaction in the localized premixed zone. The ignition source is later cutoff so the mixture must rely on the then produced heat. The self-sustaining propagation of localized combustion zone is called flame.

Flame is defined as the localized combustion zone where the chemical reactions are significant i.e. reactions rate are high. Flame thickness refers to the distance up to which the gradient in properties like mass fraction of reactants, temperature are felt. A flame travels towards the unburnt gas mixture at a speed called flame speed. In the flame fixed frame of reference, the velocity of reactants just upstream of the flame is defined as the flame speed. The unburnt reactants approach the flame with this speed. It is a unique property of a mixture, indicating its reactivity and exothermicity in a given medium. The premixed, non-premixed, laminar and turbulent nature of combustion greatly affects the nature of flame structure and flame dynamics.

Initially the complex phenomena of combustion described above will be omitted so that preliminary design parameters can be gathered using developed mathematical models assuming:

- Fuel and air is fully premixed.
- Finite rate reaction progression governed by Arrhenius Law.
- Inviscid flow
- On injecting mass, the mixing is instantaneous

(Chetiyar, 2015) designed a combustion chamber for 20 kW power production. For the purpose the paper suggested the combustor inlet parameters as follows:

Inlet Temperature	:	438.83 K
Inlet Pressure	:	2.95 bar
Mass Flow Rate of Fuel (Kerosene)	:	6.33e-3 kg/s
Kerosene Heating Value	:	43000 KJ/kg
Combustor heat production rate	:	272190 Watt

For complete combustion

Using CHCPR, the mass flow rate of air and fuel yielding the designed heat production rate on complete combustion was evaluated. The air and fuel mass flow rate are:

Air mass flow rate (m_0)	:	0.094825 kg/sec
Fuel mass flow rate (m_f)	:	0.0027827 kg/sec

4.1.1 Primary zone

4.1.1.1 Primary zone equivalence ratio

Flammability limit can be defined as the necessary equivalence ratios required for a flame to be self-supported after the ignition source is removed. In other words, the limits denote the very richest and leanest fuel concentrations possible without the flame extinguishing itself.

Table 4-1 Flammability Limits for Hydrogen in Air

	Lean	Rich	Stoichiometric
Equivalence ratio (φ)	0.1	7	1

(Jensen, 2011)

Minimum ignition energy for hydrogen/air mixture is found at approximately stoichiometric ratio at 0.95 (Nakaya et al., 2006). Richer fuel mixture associates with longer length of combustion chamber so the primary zone equivalence ratio is taken 1.2 as the richest limit where the highest combustion temperature is slightly lower than that in the case of stoichiometric combustion.

4.1.1.2 Primary zone velocity

Blowout refers to situations where the flame becomes detached from the location where it is anchored and is physically ‘‘blown out’’ of the combustor. When the opposing burning velocity cannot keep up with the unburnt gas velocity the flame blows-off. It is basically the situation where the unburnt gases does not get enough residence time for combustion.

It is believed that a smaller flame holder would create sufficient flow reversal to stabilize the flame front. Presence of a small flame holder provides enough residence time for the gases to burn in relatively smaller length. A reduction in the combustor’s length decreases the static pressure loss across the combustion chamber.

A second issue is flashback, where the flame propagates upstream of the region where it is supposed to anchor and into premixing passages that are not designed for high temperatures. Flame propagation speed is increased from the laminar flame speed S_L to the turbulent flame speed S_T. So highly turbulent flow fields provide the worst-case scenarios for flashback due to turbulent flame propagation in the core flow. This drop may become critical if the velocity field has strong wake, high turbulence regions from, e.g., swirler vanes, upstream separation zones and fuel jets.

(Lieuwen et al., 2008)

So, for flashback prevention the inlet mixture velocity is not exceeded less than 10m/sec.

Primary zone initial conditions

Temperature	:	438.83 K
Pressure	:	2.95 bar
Average equivalence ratio	:	1.2
Air mass flow rate (m_0)	:	0.079021 kg/sec
Fuel mass flow rate (m_f)	:	0.0027827 kg/sec
Density of the mixture at primary zone inlet (ρ_{mix})	:	1.69064 kg/sec
Axial velocity	:	10 m/sec
Area of flame tube (A_{ft})	:	5.0923e-3 m^3

Diameter of flame tube (D_{ft}) : 80 mm

Diameter of combustor casing (D) : 80/0.7 mm

First the combustor test case is started on PRFM assuming the case is a premixed finite rate combustion system. PRFM only works for auto-ignition. For hydrogen-air mixture, auto-ignition temperature is around 800 K. The initial mixture being at 438.83 K, it will not auto-ignite to give equilibrium products. Even for the temperature of 800 K the auto-ignition delay is about 13 seconds (from CHCPR), which requires large computation time. So, for simplicity, primary zone combustion is modelled at initial temperature of 1200 K assuming that the products' mole fraction after combustion of 483.83 K initial mixture is same as the products' mole fraction on combustion of 1200 K initial mixture, continuity being valid. Then the temperature and velocity of product mixture on combustion of 483.83 K initial mixture is calculated on the basis of mass and energy conservation.

Table 4-2 Calculation of Primary zone exit conditions on combustion of ϕ=1.2, 438.83 K, 2.95 bar hydrogen-air mixture

	Case 1	Case 2	Remarks
Initial Mixture	Phi=1.2, H_2-air	Phi=1.2, H_2-air	-
Initial Temperature	438.83 K	1200 K	-
Initial Density	1.6064 kg/m^3	0.5875 kg/m^3	From CHCPR
Initial Velocity	10 m/sec	27.343 m/sec	Continuity
Final Mixture	Same as Case 2	From PRFM	-
Final Temperature	?	2696.3 K	-
Final Velocity	?	55.0457 m/sec	-

Combustion is modelled using Case 2 in PRFM, the final temperature and velocity of Case 1 is calculated afterwards. The excess thermal and kinetic energy required to convert 438.83 K, phi=1.2 hydrogen-air mixture to 1200 K, phi=1.2 hydrogen-air mixture is subtracted from the final thermal and kinetic energy of Case 2. Continuity being valid, the final temperature and velocity of Case 1 can be calculated.

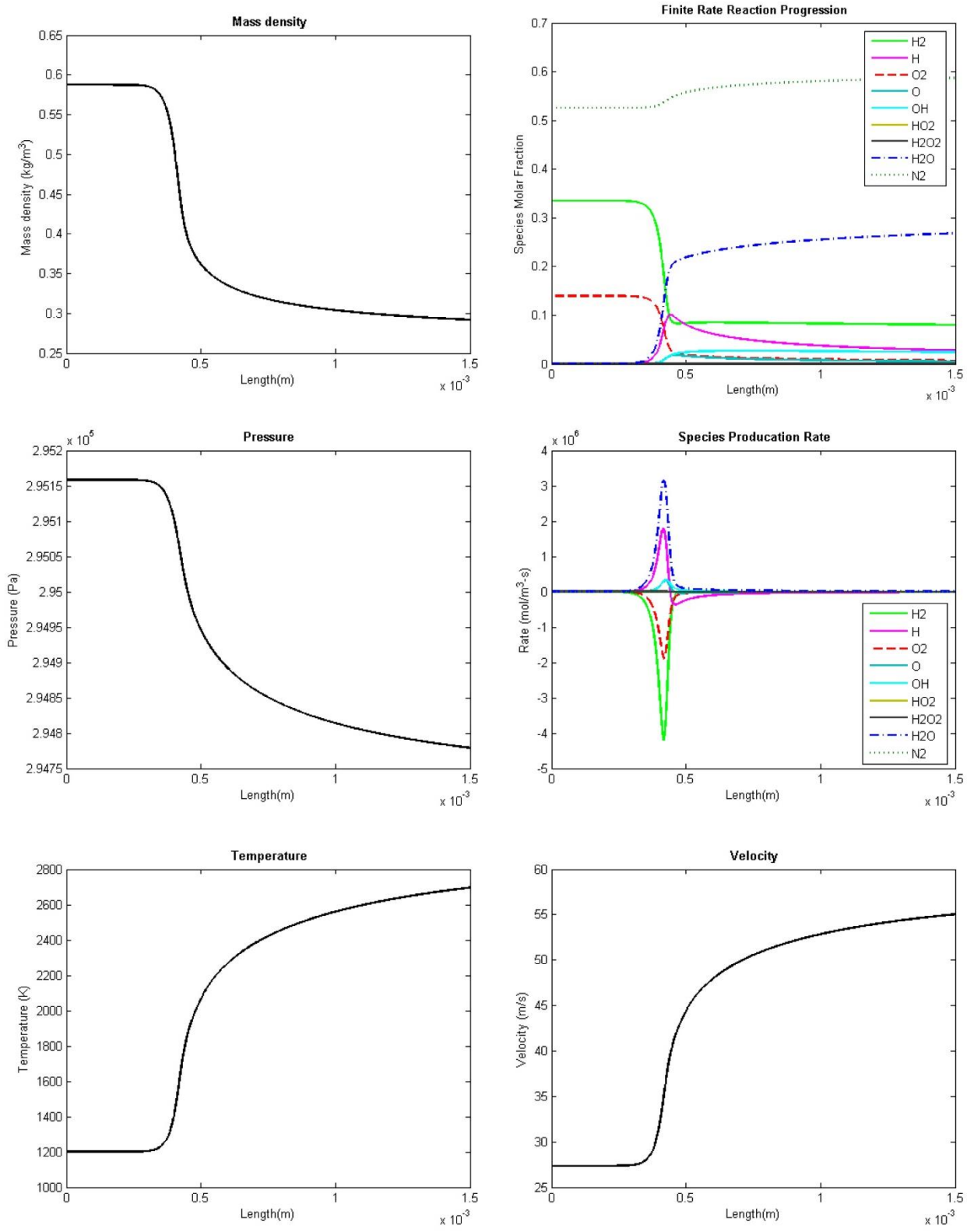

Figure 4-1 Reaction progression with length for ϕ=1.2, 1200 K, 2.95 bar, 27.343 m/sec hydrogen-air mixture (Case 2) using PRFM

Results

Table 4-3 Primary zone exit mole fractions

H_2	0.0803
H	0.0278
O_2	0.0072
O	0.0053
OH	0.0242
HO_2	$6.1894*10^{-6}$
H_2O_2	$1.2691*10^{-6}$
H_2O	0.2682
N_2	0.5870

Primary zone exit temperature : 1970.65 K

Primary zone exit velocity : 40.188 K

Primary zone exit density : 0.39972 kg/m^3

4.1.2 Secondary and Dilution zones

The final mole fractions, temperature, velocity of the primary zone is fed as initial condition for secondary and dilution zones. For estimating the total mass flow entering combustor in secondary and dilution zone, the combustor outlet total temperature is considered as design parameter. The total mass flow rate of air that is injected through curved surface area of the flame tube to dilute the combustor exit temperature to 1600 K is estimated using PRFM. First to estimate total mass flow for secondary and dilution zones an arbitrary mass injection flux is defined. The mass flux injected is integrated along the length by PRFM. The mass flow injection at the length at which the total temperature becomes 1600 K is the estimated mass flow for secondary and dilution zones.

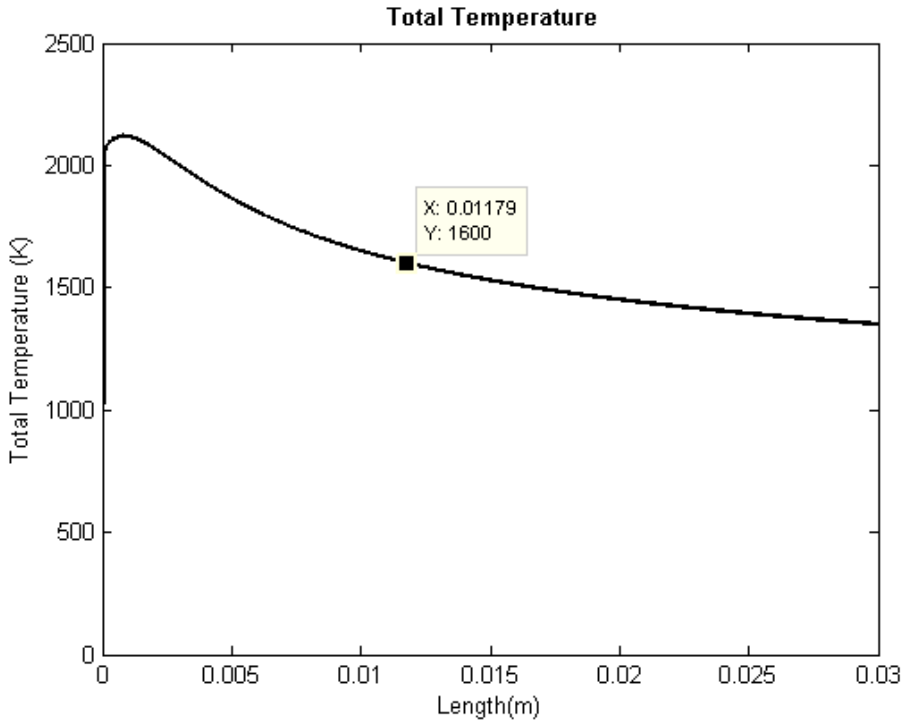

Figure 4-2 Total temperature with length upon air injection at constant mass flux of 95.571 kg/m^2/sec in Primary zone exit conditions

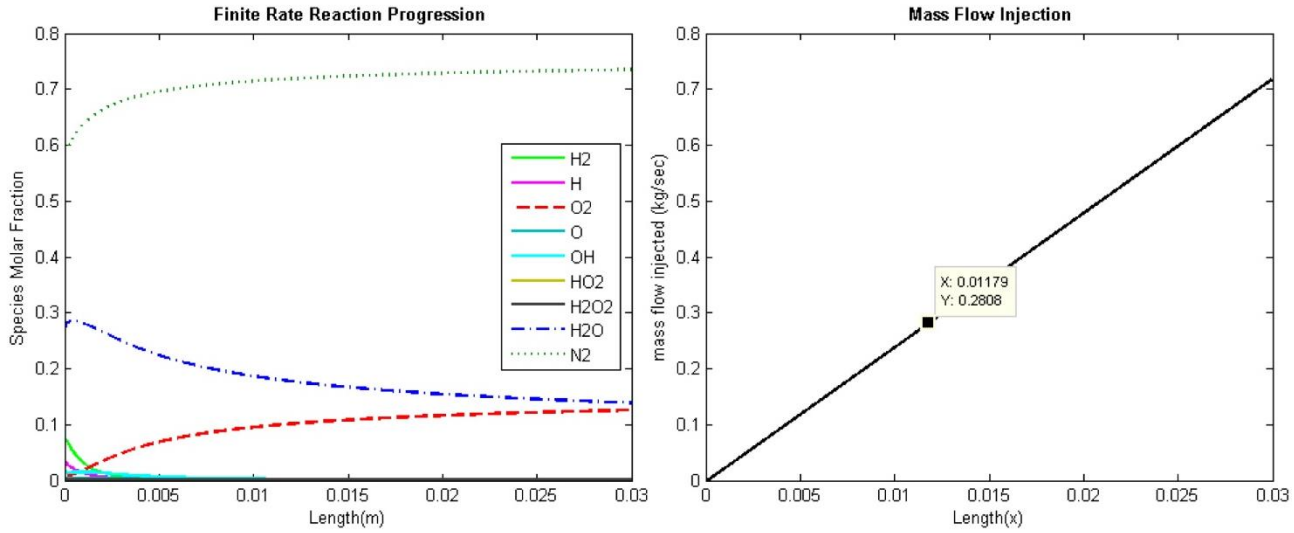

Figure 4-3 Reaction progression and mass flow injection with length upon air injection at constant mass flux of 95.571 kg/m^2/sec in Primary zone exit conditions

Knowing the mass flow rate for secondary and dilution zones, the actual mass flow rate for secondary and dilution zones is input to the PRFM as air flow over flame tube to estimate secondary and dilution zones' port dimensions. Air runs over the flame tube in the conduit between flame tube (D_{ft}) and combustor casing (D). The mass flux over the flame tube is set constant through gradual reduction of chamber's diameter, diameter of the flame tube held constant. Air enters inside the flame tube with the same flux. The length of secondary and dilution ports along with the mass flow required for both secondary and dilution zones is estimated using PRFM evaluations.

Initial Cross-sectional Area of air flowing over flame tube:

$$\text{Area} = \frac{\pi}{4}\left[\frac{0.08}{0.7}\right]^2 - \frac{\pi}{4}0.08^2 = 0.005232\ \text{m}^2$$

Combustor exit total temperature : 1600 K

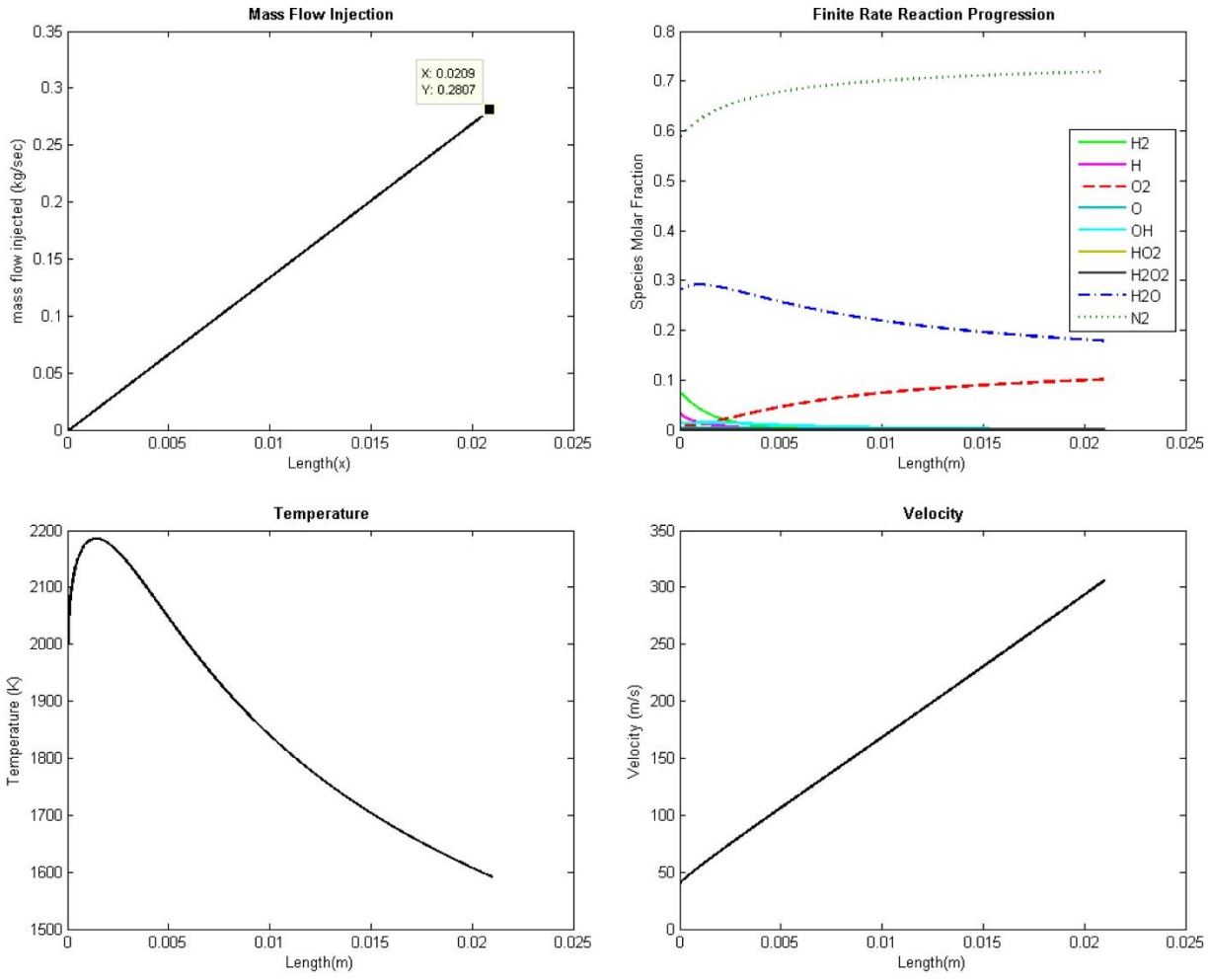

Figure 4-4 Variation of mixture properties on air injection at mass flux of 53.6727 kg/m^2/sec

Mass flow rate over the flame tube	:	0.2808 kg/sec
Mass flux associated with air injection	:	53.6727 kg/m^2/sec

From the plots **(Figure 4-4)**, the length required for complete reaction of spare hydrogen molecules is stated as the length of secondary zone port and the respective mass flow rate as the secondary mass flow rate. The length and mass flow rate required to further dilute the gases to the combustor exit temperature of 1600 K is the estimation of length of dilution zone's port and the respective mass flow rate.

Taking 0.01m **(Figure 4-4)** as the length required for excess hydrogen fuel to react giving stable products, the secondary air inlet port length is selected as 0.01 m. So the further mass flow required to dilute the combustor gases to 1600 K is selected as dilution mass flow.

Secondary air inlet mass flow rate	:	0.1337 kg/sec
Secondary air inlet port length	:	0.01 m
Dilution air inlet mass flow rate	:	0.1471 kg/sec
Dilution air inlet port length	:	0.011 m

Knowing the primary zone inlet conditions, secondary and dilution zone's port dimensions and respective mass flow rates, the design of combustor is further continued in ANSYS Fluent.

4.1.3 Geometry and flow configuration

The Gas Combustor Test Case is further continued in ANSYS Fluent using the primary zone inlet conditions, secondary zone and dilution zone conditions. The model setup and boundary conditions are as follows:

Model Setup

Energy	:	On
Viscous	:	Standard k-e, Standard Wall Fn
Radiation	:	Off
Heat Exchanger	:	Off

Species Transport	:	Hydrogen-Air mixture
Reaction	:	Volumetric
Turbulence-Chemistry Interaction	:	Eddy-Dissipation
Diffusive Energy Source	;	On
Two Dimensional Space	:	Axisymmetric Swirl
Time	:	Steady

Boundary Conditions

Air Inlet	:	Mass flow inlet
Fuel Inlet	:	Mass flow inlet
Secondary, Primary, Dilution	:	Mass flow inlet or wall
Wall	:	No slip wall with zero heat flux
Axis	:	Axis

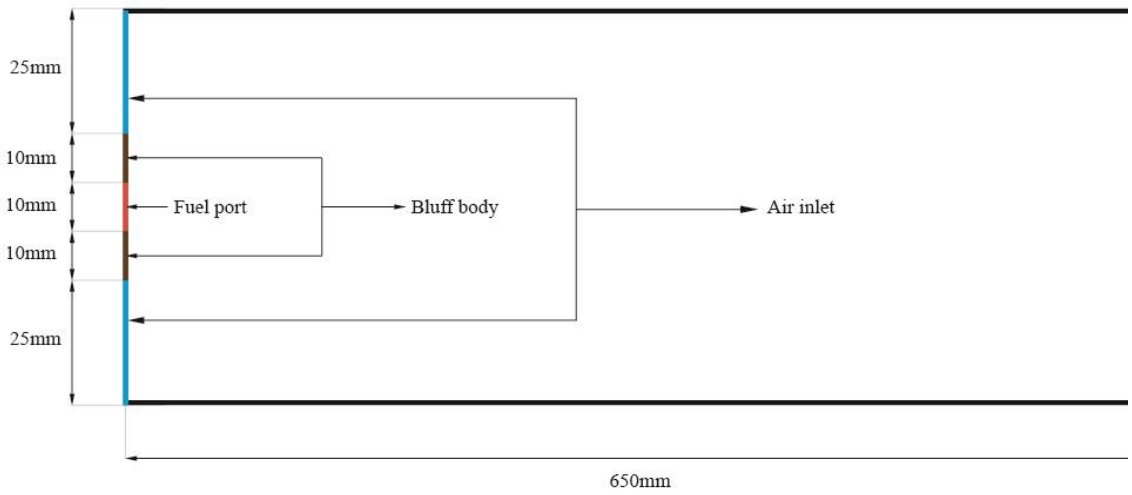

Figure 4-5 Model geometry

First, the primary zone air and fuel mass flow along with thermodynamic properties like temperature, pressure, mole fraction were given as boundary conditions at the designated parts.

Conditions being

Air inlet

Mass flow rate	:	7.9021e-2
Temperature	:	438.83 K
Pressure	:	2.95 bar
Mole Fraction	:	21% Oxygen and 79% Nitrogen

Fuel port

Mass flow rate	:	2.7827e-3
Temperature	:	300 K
Pressure	:	2.95 bar
Mole Fraction	:	100% hydrogen

Bluff body : No slip wall

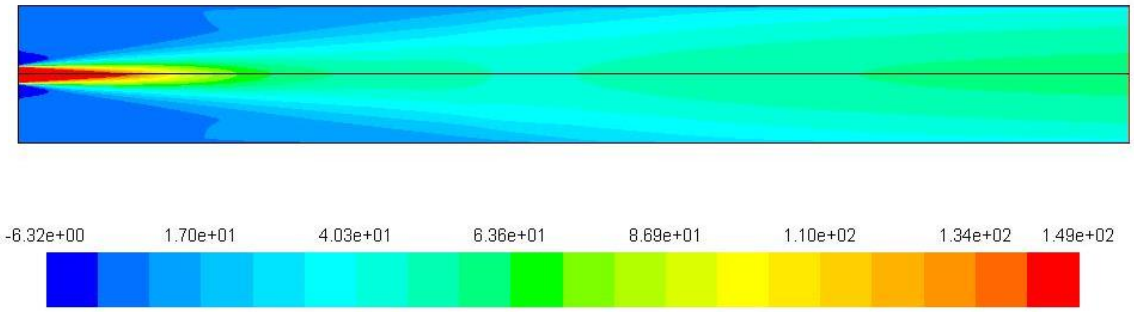

Figure 4-6 Axial velocity contour (m/sec)

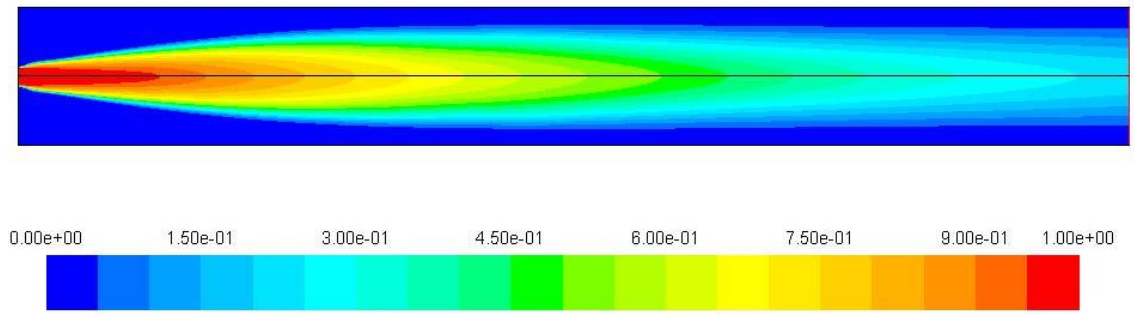

Figure 4-7 Hydrogen mole fraction contour

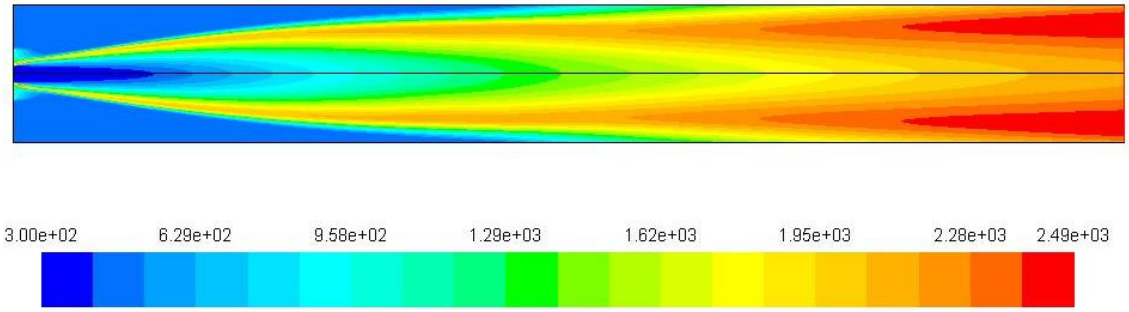

Figure 4-8 Temperature contour (K)

The velocity of fuel is found at the range of 150 m/sec, which allowed less mixing time of fuel in the combustor.

To increase fuel mixing time a recirculation zone was created with the help of swirl and radial component of air and fuel mass flow.

Air inlet directional vector

Axial	:	1
Radial	:	-1
Tangential	:	3

Fuel flow directional vector

Axial	:	1
Radial	:	0
Tangential	:	-2

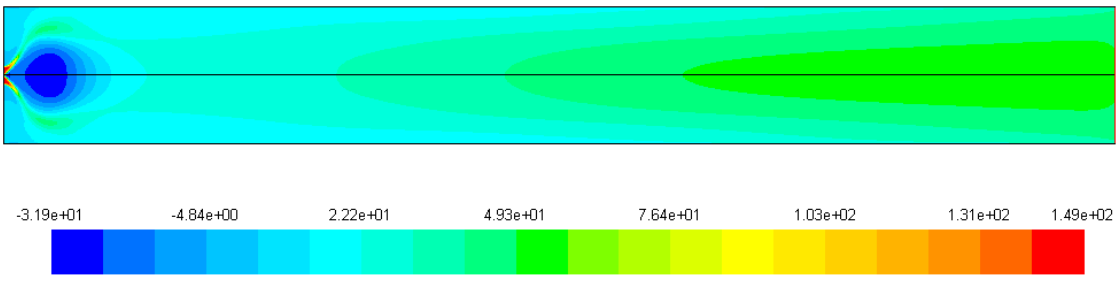

Figure 4-9 Axial velocity contour upon swirl and radial air and fuel flow components

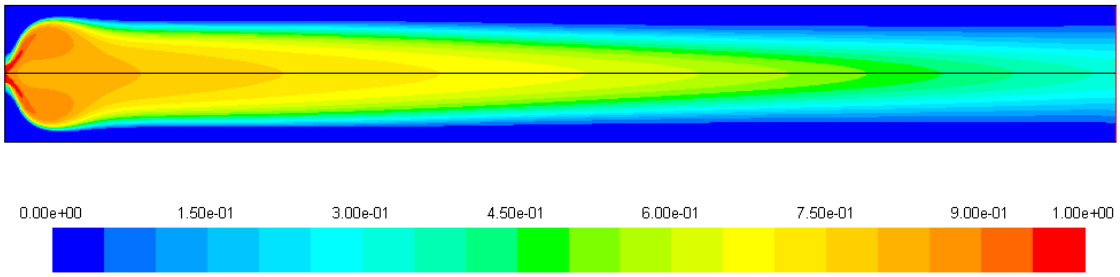

Figure 4-10 Hydrogen mole fraction contour upon swirl and radial air and fuel flow components

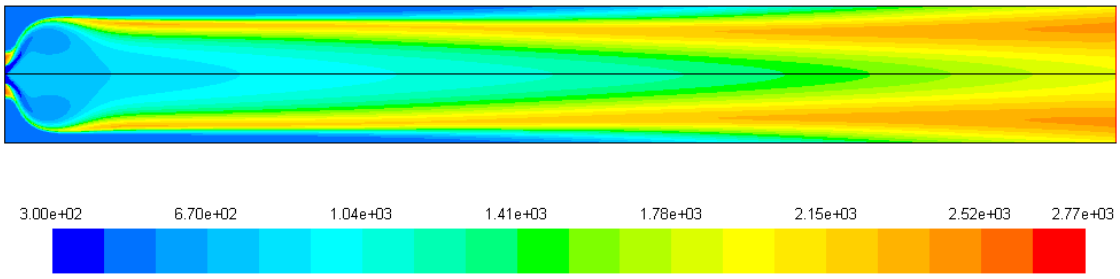

Figure 4-11 Temperature contour upon swirl and radial air and fuel flow components

Then, in the setup secondary mass flow was introduced just aft of recirculation zone.

Secondary air inlet mass flow rate	:	0.1337 kg/sec
Secondary air inlet port length	:	0.01 m

Secondary zone inlet mass flow was divided proportionally such that 30% is injected through wall at the axial distance of 40 mm and 70 % at the axial distance of 100mm through proportionally divided ports.

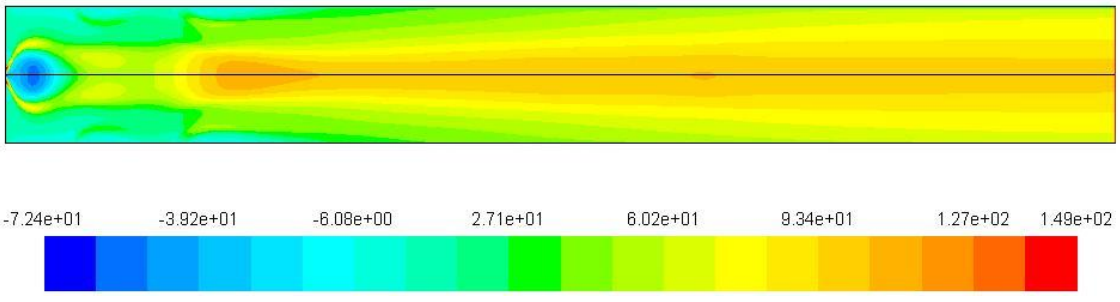

(a)

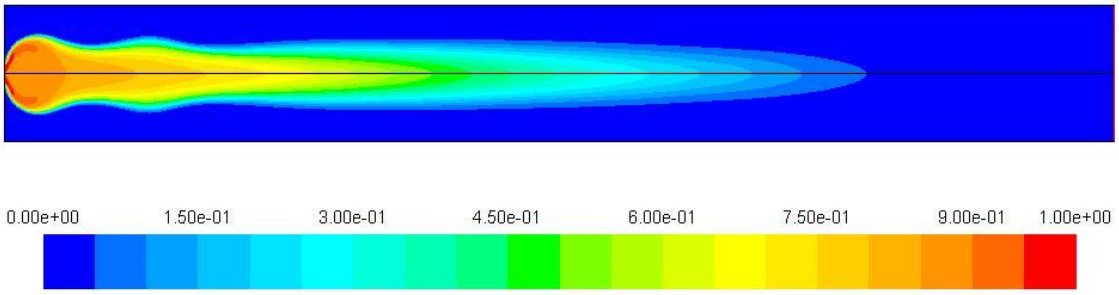

(b)

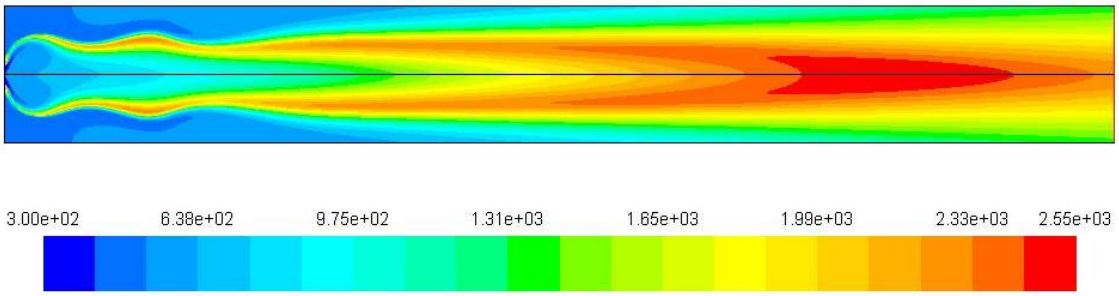

(c)

Figure 4-12 (a) Axial velocity, (b) Hydrogen mole fraction, (c) Temperature contour upon swirl and radial air and fuel flow components with 30% of secondary air injected through wall at the axial distance of 40 mm and 70 % at the axial distance of 100mm

Then remains the position of dilution mass inlet.

A case where:

Secondary air inlet mass flow rate	:	0.1337 kg/sec
Secondary air inlet port length	:	0.01 m
Dilution air inlet mass flow rate	:	0.1471 kg/sec
Dilution air inlet port length	:	0.011 m

were injected through wall at the position of 40 mm and 100 mm respectively.

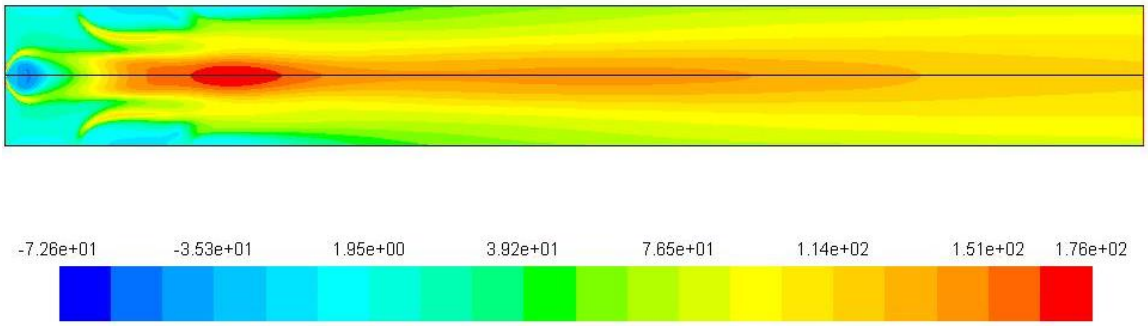
-7.26e+01
-3.53e+01
1.95e+00
3.92e+01
7.65e+01
1.14e+02
1.51e+02
1.76e+02

(a)

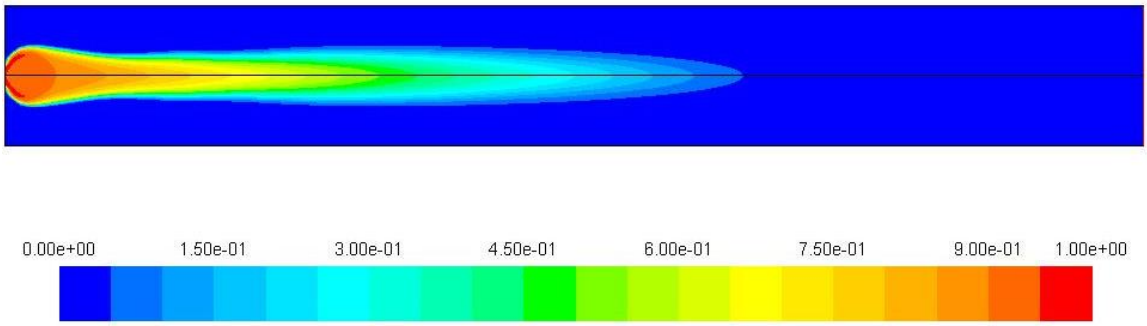
0.00e+00
1.50e-01
3.00e-01
4.50e-01
6.00e-01
7.50e-01
9.00e-01
1.00e+00

(b)

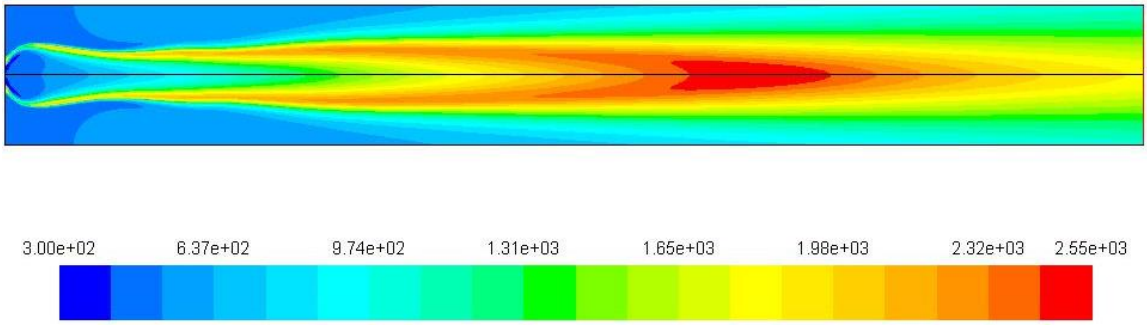
3.00e+02
6.37e+02
9.74e+02
1.31e+03
1.65e+03
1.98e+03
2.32e+03
2.55e+03

(c)

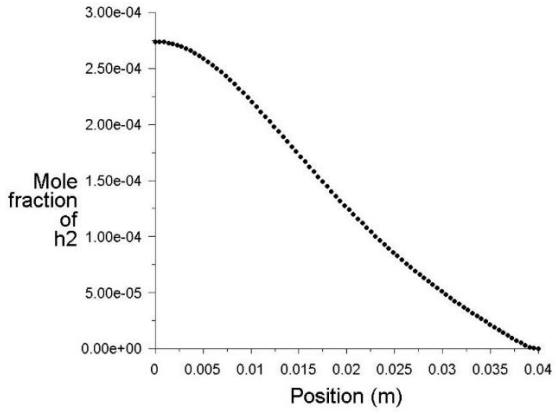
Mole fraction of h2
3.00e-04
2.50e-04
2.00e-04
1.50e-04
1.00e-04
5.00e-05
0.00e+00
0
0.005
0.01
0.015
0.02
0.025
0.03
0.035
0.04
Position (m)

(d)

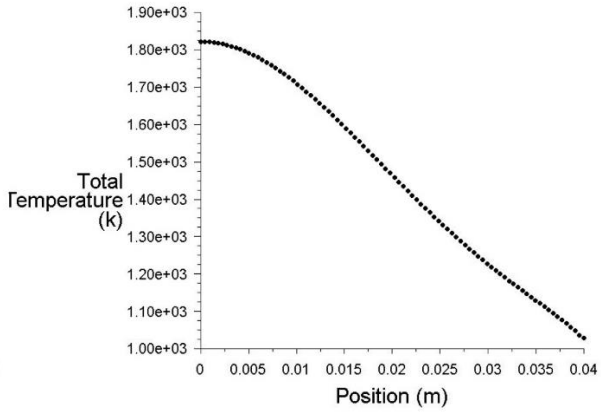
Total Temperature (k)
1.90e+03
1.80e+03
1.70e+03
1.60e+03
1.50e+03
1.40e+03
1.30e+03
1.20e+03
1.10e+03
1.00e+03
0
0.005
0.01
0.015
0.02
0.025
0.03
0.035
0.04
Position (m)

(e)

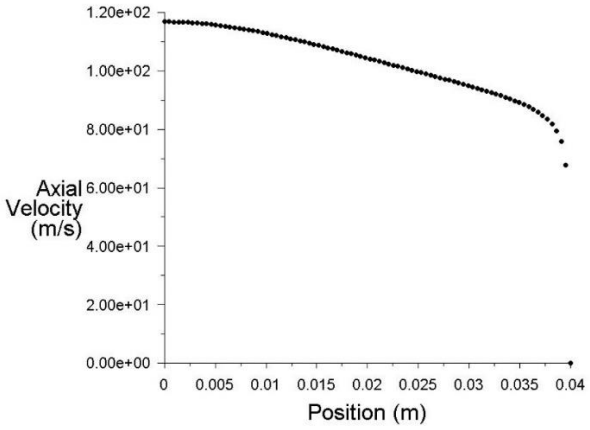

(f)

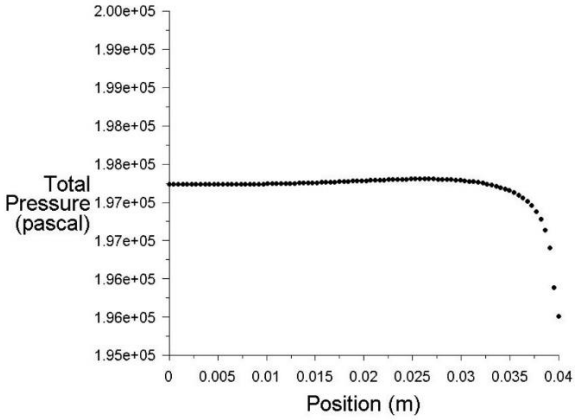

(g)

Figure 4-13 (a) Axial velocity contour, (b) Hydrogen mole fraction contour, (c) Temperature contour, (d) Outlet hydrogen mole fraction profile, (e) Outlet total temperature profile, (f) Outlet axial velocity profile, (g) Outlet total pressure profile, upon swirl and radial air and fuel flow components with secondary air injected through wall at the axial distance of 40 mm and dilution air at the axial distance of 100mm

Upon early injection of dilution air mass prior to complete reaction of hydrogen fuel, the fuel stream tube converged along with addition of mass such that the unreacted hydrogen stream at the centerline accelerated reducing mixing time and fuel residence time. The case also showed the possibility of reduction of wall temperature upon injecting air significant axial positions apart.

Finally, the dilution zone air inlet was positioned at 250 mm axial distance.

The setup being:

Secondary air inlet mass flow rate	:	0.1337 kg/sec
Secondary air inlet port length	:	0.01 m

divided proportionally such that 30% is injected at the axial distance of 40 mm and 70 % at the axial distance of 100 mm through proportionally divided ports.

Dilution air inlet mass flow rate	:	0.1471 kg/sec
Dilution air inlet port length	:	0.011 m

injected through wall at 250 mm axial distance.

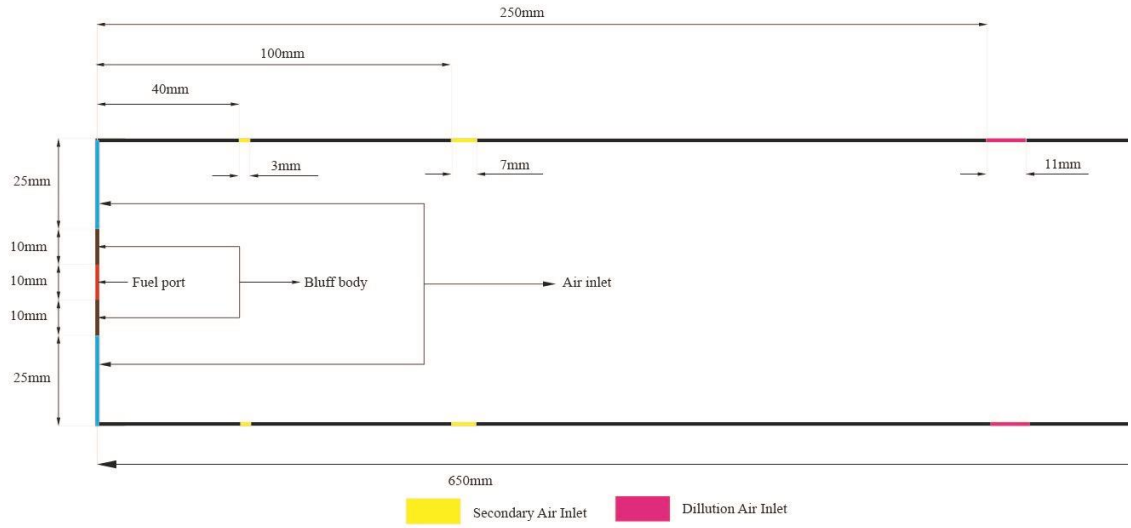

Figure 4-14 Final combustor configuration illustration

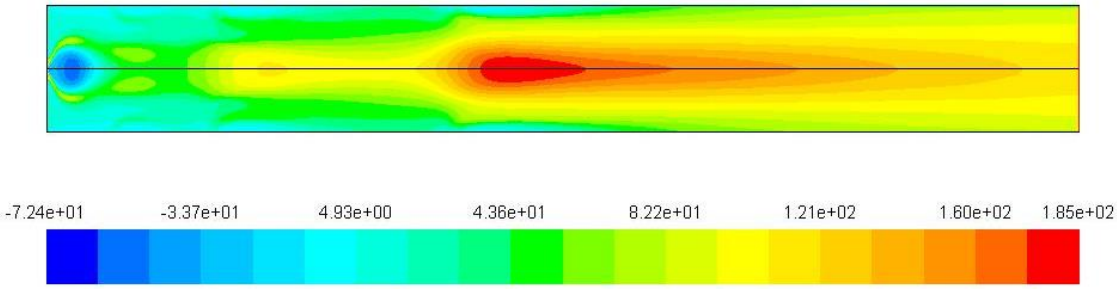

(a)

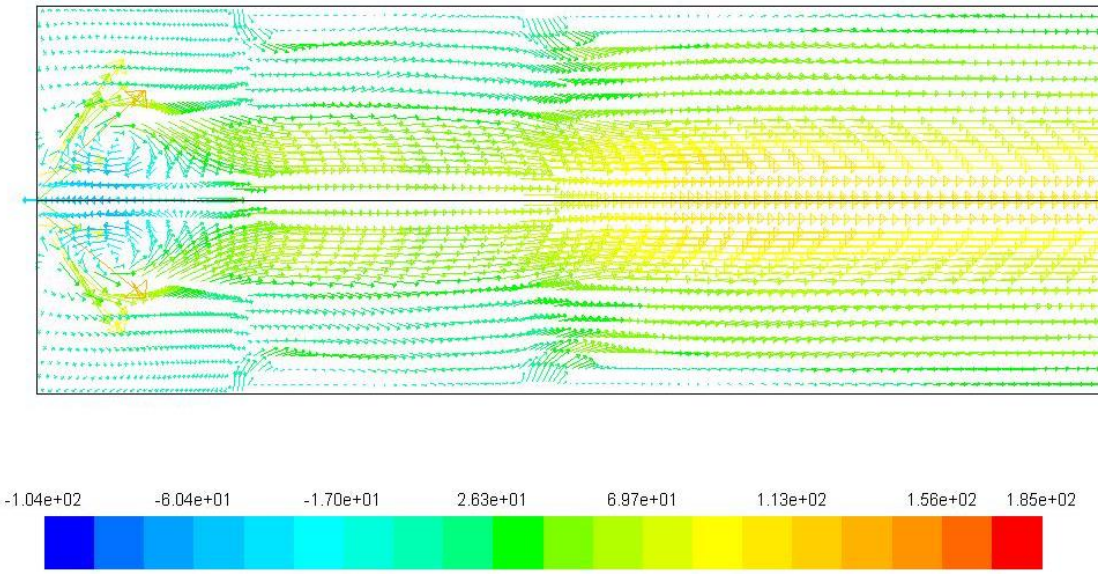

(b)

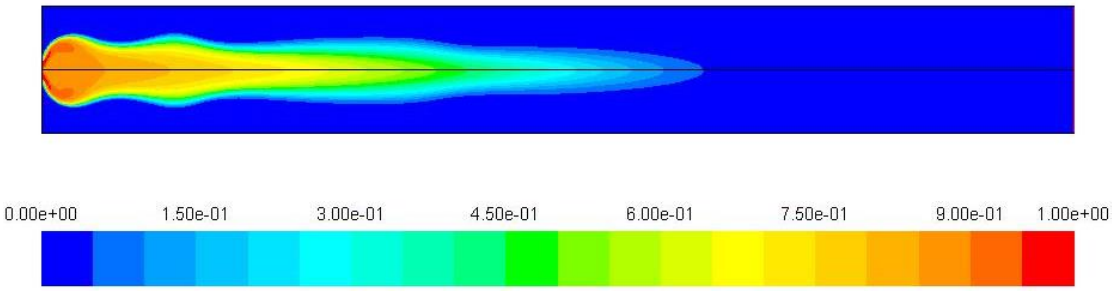
0.00e+00
1.50e-01
3.00e-01
4.50e-01
6.00e-01
7.50e-01
9.00e-01
1.00e+00

(c)

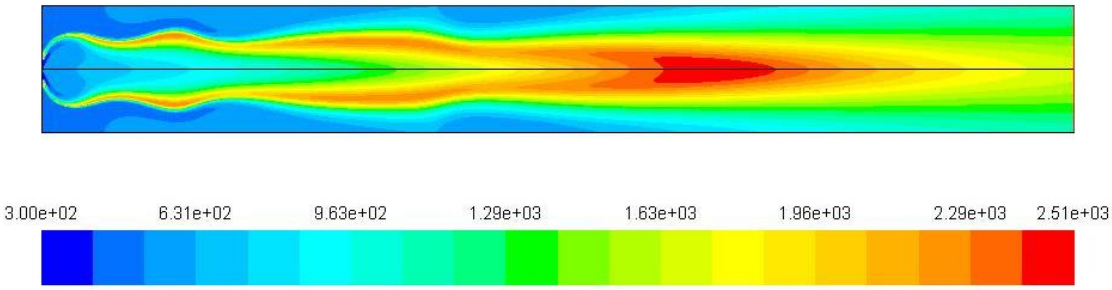
3.00e+02
6.31e+02
9.63e+02
1.29e+03
1.63e+03
1.96e+03
2.29e+03
2.51e+03

(d)

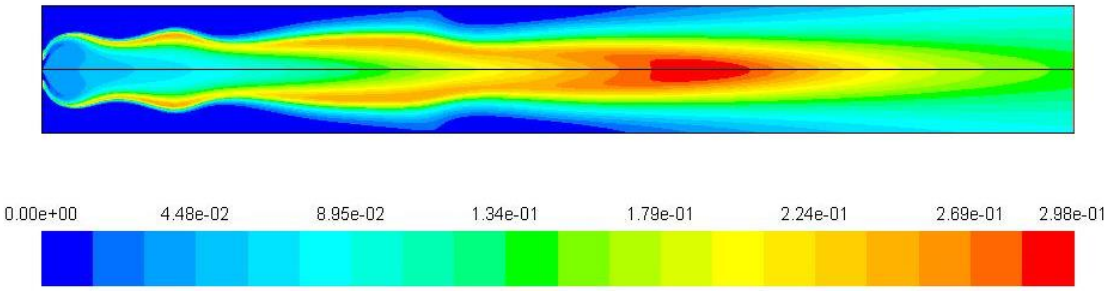
0.00e+00
4.48e-02
8.95e-02
1.34e-01
1.79e-01
2.24e-01
2.69e-01
2.98e-01

(e)

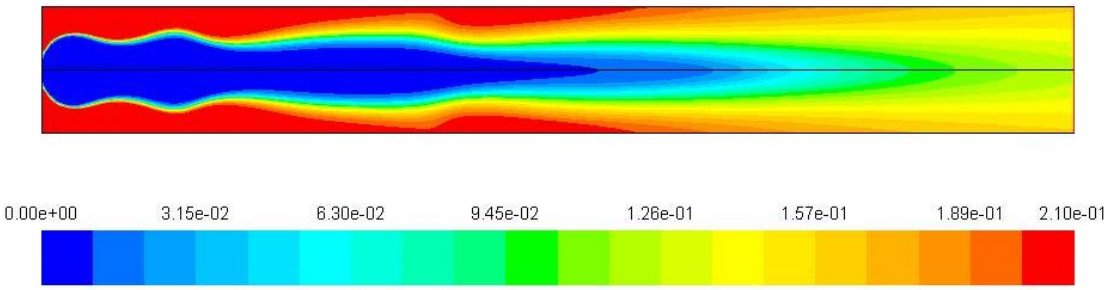
0.00e+00
3.15e-02
6.30e-02
9.45e-02
1.26e-01
1.57e-01
1.89e-01
2.10e-01

(f)

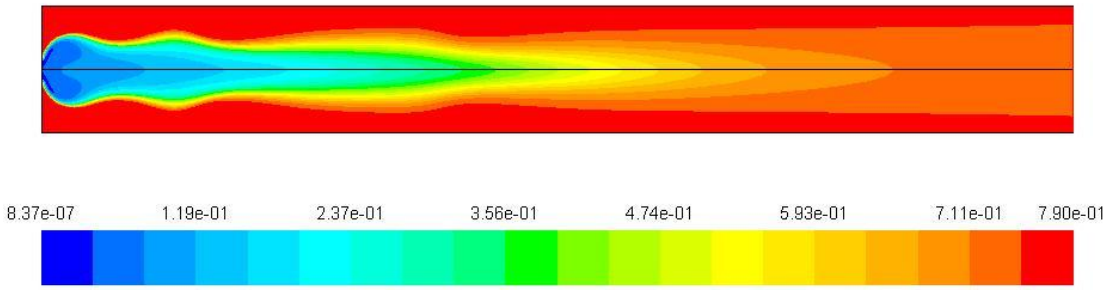

(g)

Figure 4-15 (a) Axial velocity contour, (b) Axial velocity vector, (c) Hydrogen mole fraction, (d) Temperature contour, (e) H_2O, (f) O_2, (g) N_2 mole fraction upon swirl and radial air and fuel flow components with 30% of secondary air injected through wall at the axial distance of 40 mm and 70 % at the axial distance of 100mm and dilution air at the axial distance of 250mm

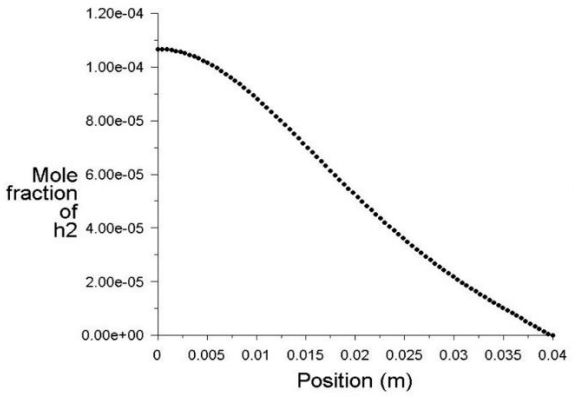

(a)

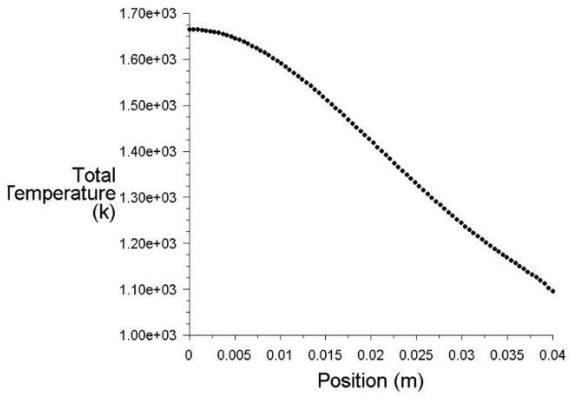

(b)

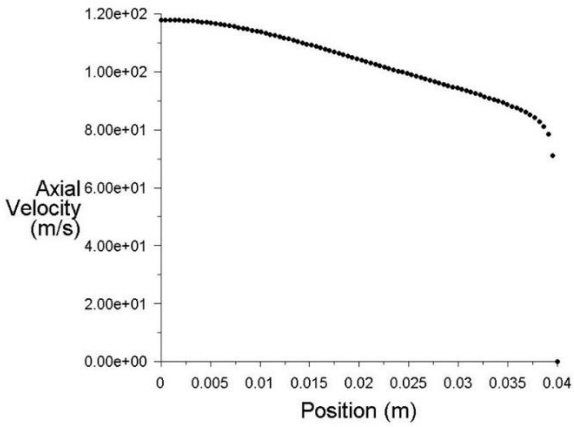

(c)

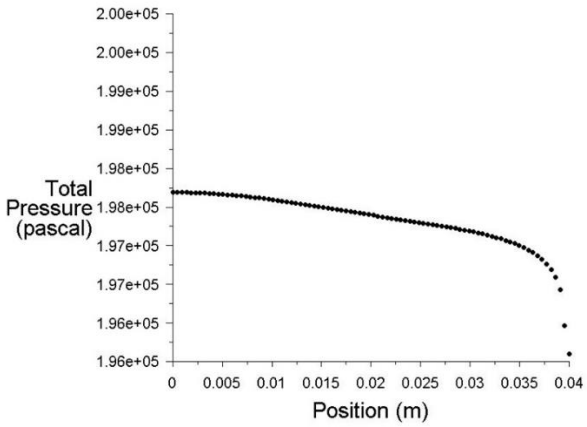

(d)

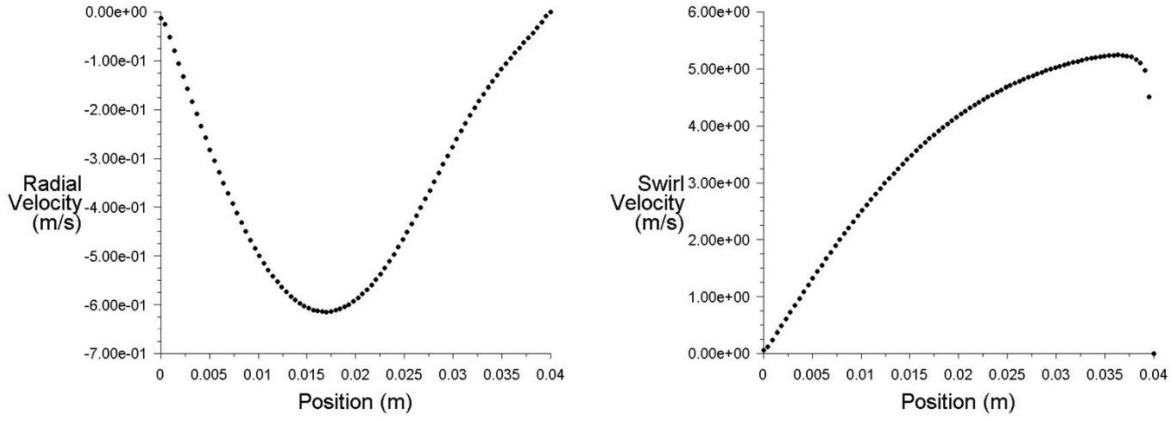

(e) **(f)**

Figure 4-16 (a) Hydrogen mole fraction profile, (b) Total Temperature, (c) Axial velocity, (d) Total pressure, (e) Radial velocity, (f) Swirl velocity, profile at outlet, upon swirl and radial air and fuel flow components with 30% of secondary air injected through wall at the axial distance of 40 mm and 70 % at the axial distance of 100mm and dilution air at the axial distance of 250mm

4.1.4 Results and Conclusions

The combustion and dilution characteristics of hydrogen-air mixture in a slender combustion tube was studied. The bluff body wall provided stagnating boundary layer combustion surface that remained maintained at higher temperature acting as flame holder **(Figure 4-15 d)**. Air and fuel swirl and radial velocities created recirculation zone near fuel injector that enhanced mixing also adding to flame-holding characteristics **(Figure 4-15 b)**. The secondary and dilution zone air inlet were separated certain axial distance apart such that dilution air is injected after hydrogen fuel is completely consumed. The separation helped to abate tactility of flame with wall, comparing **(Figure 4-13 c)** and **(Figure 4-15 d)**, that helped in minimizing wall temperature along the length of the combustor and to limit axial velocity of centerline stream consisting unreacted gases increasing fuel residence time, comparing **(Figure 4-13 a)** and **(Figure 4-15 a)**. The mixing was also seen enhanced on the separation, as total temperature profile on the separation was found more uniform comparing **(Figure 4-13 e)** and **(Figure 4-16 b)**. The total pressure at outlet was also higher in latter case **(Figure 4-13 g)** and **(Figure 4-16 d)**. The predefined combustor exit total temperature of 1600 K was met at a combustor length of 650 mm **(Figure 4-16 b)**.

On concluding remarks, the mathematical models based on simplified flow dynamics and detailed chemical reaction can also be used for preliminary design of practical combustion systems. Acknowledging the predefined assumption, valuable combustion

and chemical kinetics characteristics of a practical system can be formulated using the mathematical models developed and described in the thesis.

4.2 Premixed Fuel-Air Flow

4.2.1 Mathematical formulation

(Figure 4-17) shows the cross-sectional view of a typical two-dimensional cylindrical combustion chamber. All dimensions are in millimeter. In this channel burning of hydrogen and air takes place. In this figure, x-axis denotes the longitudinal direction and y-axis denotes the transverse direction. Premixed hydrogen-air mixture flows along the positive x-direction at relatively slow speed and pressure remains almost constant during chemical reaction. The flow is considered to be steady and axis-symmetric which renders the problem 2D symmetric. By certain design and computational assumptions the swirl component of velocity is taken as zero. The computations are performed only in half of the domain for the sake of economic usage of computational time. The following assumptions are also invoked to further simplify the problem:

- No work is done by pressure and viscous forces.
- Wall is insulated
- No gas radiation occurs
- Soret and DuFour's effect is neglected
- Body forces are negligible
- No energy source term
- Chemical reaction occurs in a single step.
- Low Mach number

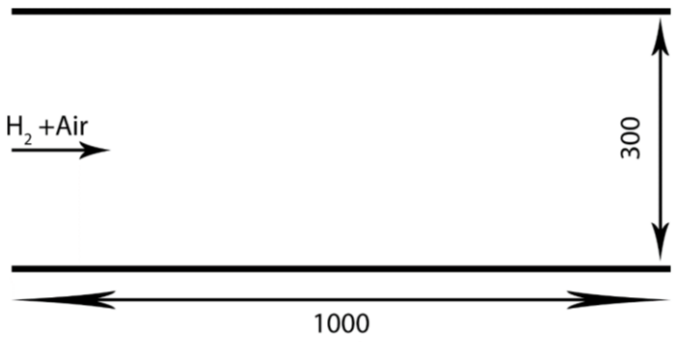

Figure 4-17 Schematic of the 2D computational domain of a cylindrical combustion chamber

4.2.2 Boundary conditions

The boundary conditions are as follows:

Inlet:

At inlet (x = 0): Temperature (T) = 1000K, inlet velocity (u) = 10 m/s. ϕ = 0.2 to 5. Mass fractions for hydrogen and oxygen can be derived from equivalence ratio.

Gas–solid interface (wall):

No slip boundary condition at the walls. Wall is insulated.

4.2.3 Results and Discussion

4.2.3.1 Simulation results at ϕ = 1.88

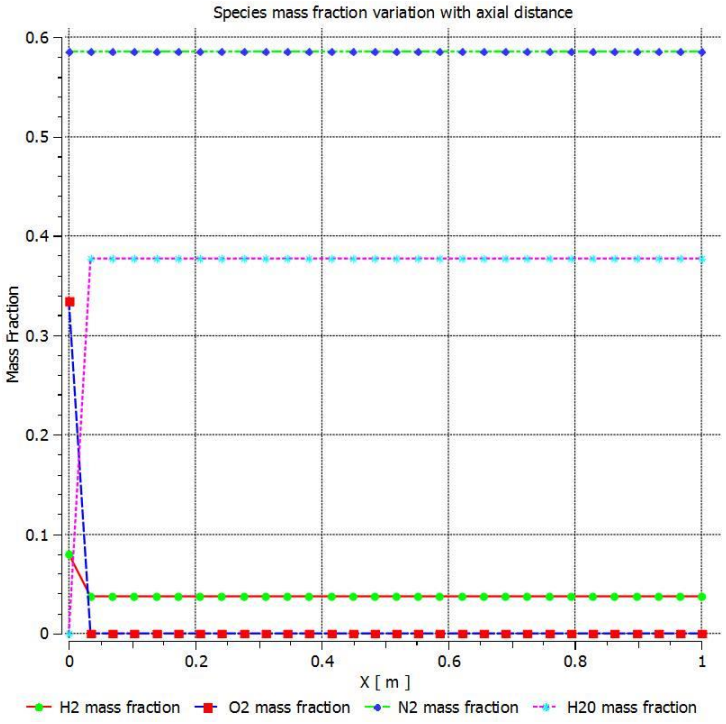

Figure 4-18 Species mass fraction variation with axial distance

(Figure 4-18) shows the variations of mass fraction of species along the axial length of the cylindrical combustion chamber. The reaction has happened so fast that at the length scale of around 0.03 meters, all the available oxygen is consumed in the reaction and further reaction do not take place.

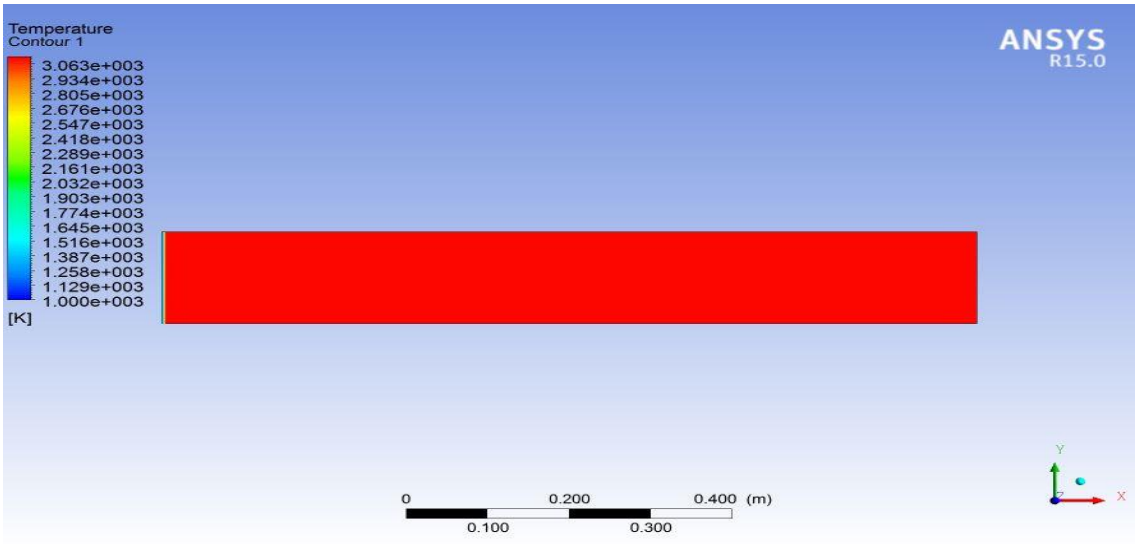

Figure 4-19 Temperature contour for ϕ = 1.88 and u=10 m/s

Due to fast reaction, most of the region of the chamber has high temperature of around 3000 K. In **(Figure 4-19)**, it is seen that whole chamber is at high temperature, but this not the case. Zooming into the inlet portion of the chamber, **(Figure 4-20)** shows the variation of temperature with axial distance.

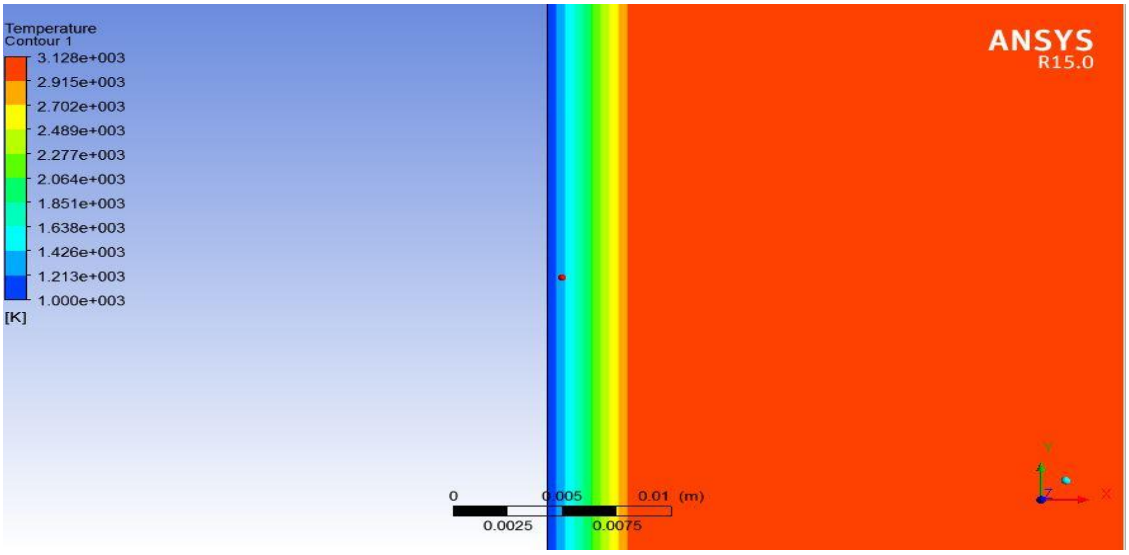

Figure 4-20 Temperature contour (zoomed in at the inlet)

4.2.3.2 Effect of equivalence ratio on flame temperature

For stoichiometric ratio ϕ=1, we see that flame has its maximum temperature**. (Figure 4-21)** shows the effect of equivalence ratio on centerline temperature of the flame. For inlet values: axial velocity (u) = 10 m/s, centerline temperature of flame for equivalence ratio 1 is maximum in comparison of centerline temperature for equivalence ratio 0.8, 1.2 and other values except 1. It means combustion zone in case of leaner and richer mixture is large to accommodate the effect of temperature. One more advantage is that we can get stable flame even on lower temperature with proper combustion of fuel. This leads to economic combustion because it opens more choices for materials to be used in combustion chambers.

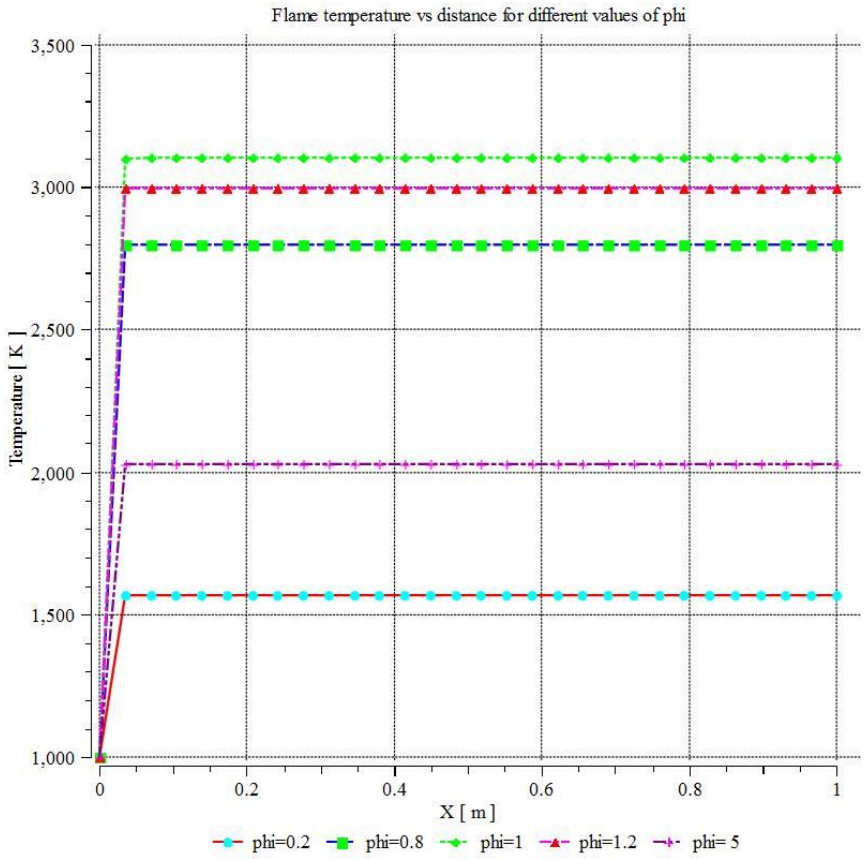

Figure 4-21 Equivalence ratio effect on the centerline flame temperature

4.3 Cavity Based Flame-Holder

Study of flame stabilization for premixed flow in recessed ducts (cavity) at subsonic speeds is presented here. In cavity stabilized combustion, a recessed duct is placed in the flow to produce a recirculating zone in it. As a result, combustion products settle there to continuously ignite fresh reactants and thus the combustion is self-sustained.

4.3.1 Geometry and flow configuration

The geometry of the combustion chamber is shown in figure given below, where all the units are in mm. The configuration used is one of the many recesses in the walls of the test chamber used at the Gas Dynamics Laboratory of Northwestern University, Evanston III.

(L.W. Huellmantel & R.W. Ziemer, 1957) used different geometries of cavity experimentally to study flame stabilization in recessed ducts.

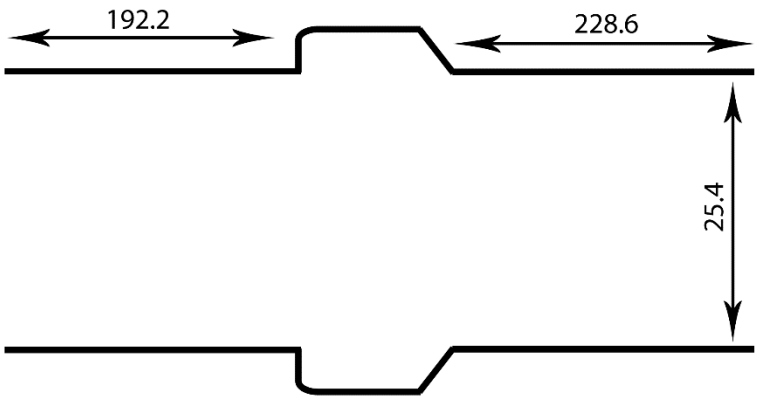

(a)

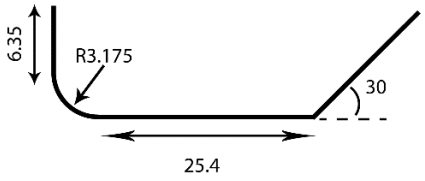

(b)

Figure 4-22 (a) Walls with recessed ducts, (b) Recessed duct enlarged with proper dimensions

The computational domain is symmetric so only a single half of the combustor was modeled.

Propane was taken as the fuel and air as oxidizer. Since air and fuel are premixed, chemical reaction can be accurately modeled by finite rate chemistry. So, Laminar/Finite rate model was used to simulate combustion in the chamber. A global mechanism was considered rather than detail chemical kinetics to minimize computation time. Transient solution was used for this case. Initial conditions for the case are presented on table below.

Table 4-4 Inlet Conditions for Cavity stabilized flame

Inlet Fuel-air mixture speed	15 m/s
Equivalence ratio at inlet	1
Pressure at outlet	1 atm
Temperature at inlet	294 K

4.3.2 Result and Discussion

From **(Figure 4-23)** and **(Figure 4-24),** recirculating zone in the cavity can be clearly seen. The streamlines inside the cavity are circulating, thus flow inside in these stream tubes have sufficient time for combustion when compared with the flow without any cavity at the wall, where streamlines are rather straight. Due to this recirculation, the effective distance which flow has to travel is increased as the streamlines are curved and thus the effective length of the combustion chamber can be decreased by the use of cavity.

(Figure 4-25) shows plot of propane mass fraction after combustion which indirectly shows a turbulent premixed flame formed at the cavity wall. It can be seen that the flame originates from the point where the step in the wall begins. The flames from the upper and lower holders then spread across the chamber as the mixture flows downstream, and eventually the two flame fronts meet. Due to comparatively lower velocity at the cavity and almost stagnant flow just behind the cavity, flame stabilization is achieved in this region and the flame seems to be anchored at the cavity wall, shown in **(Figure 4-27)**. The presence of cavity results in decreasing axial velocity at the recessed wall. So, a region of very low velocity is formed here as shown in **(Figure 4-26).**

Various detailed mechanism for propane combustion give slightly different value of adiabatic flame temperature. So for stoichiometric air fuel ratio a range of 2300 – 2400 K is reasonable adiabatic flame temperature. From the case analysis, highest temperature achieved was found to be 2356 K. Thus, an alternative method of flame stabilization is proposed in an effort to obviate the pressure drop associated with bluff body flameholders. Technologically, a flame such as this which occurs adjacent to the walls may be somewhat undesirable because of the drastic heating effects which would prove to be quite detrimental in an engine. However, the technique of using wall flameholders does offer certain possibilities in practice as well as in laboratory studies.

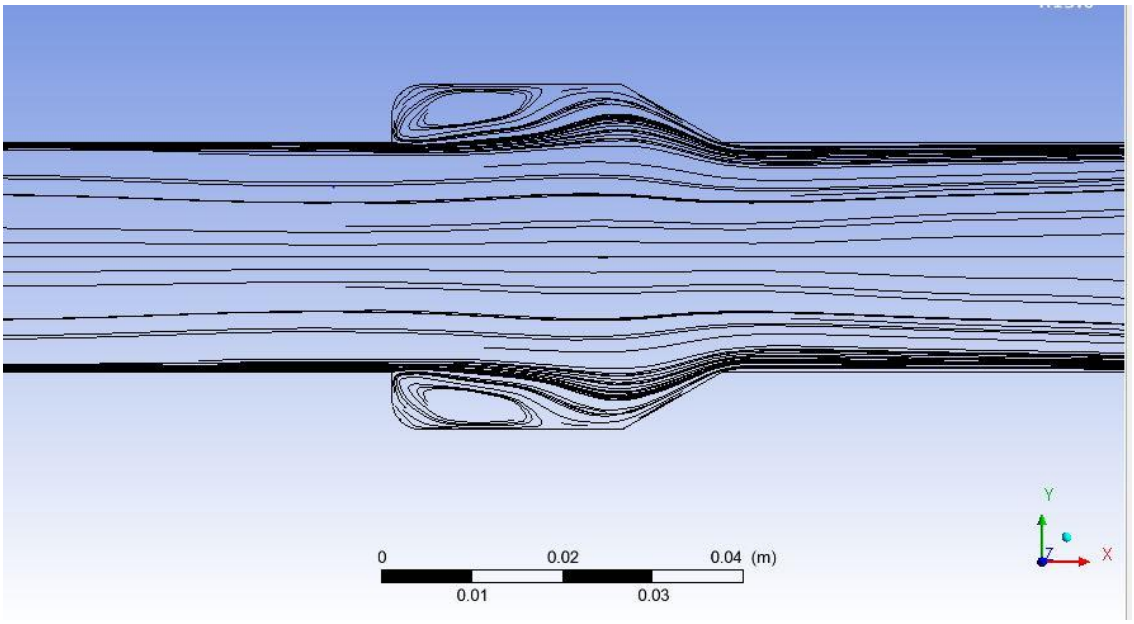

Figure 4-23 Streamlines in reacting flow

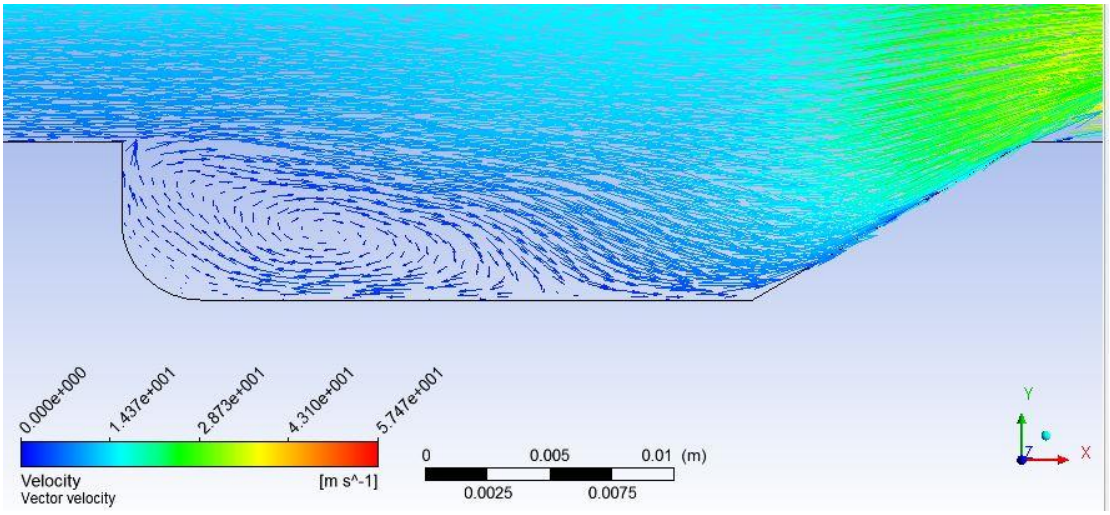

Figure 4-24 Velocity vector in reacting flow zoomed at the cavity

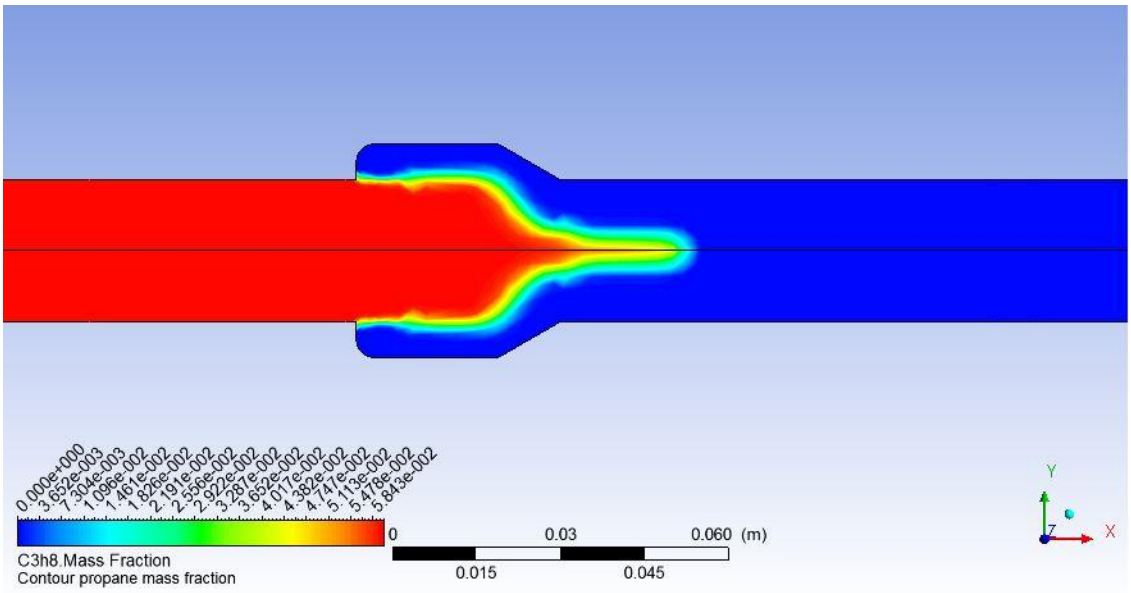

Figure 4-25 Contours of propane mass fraction after combustion

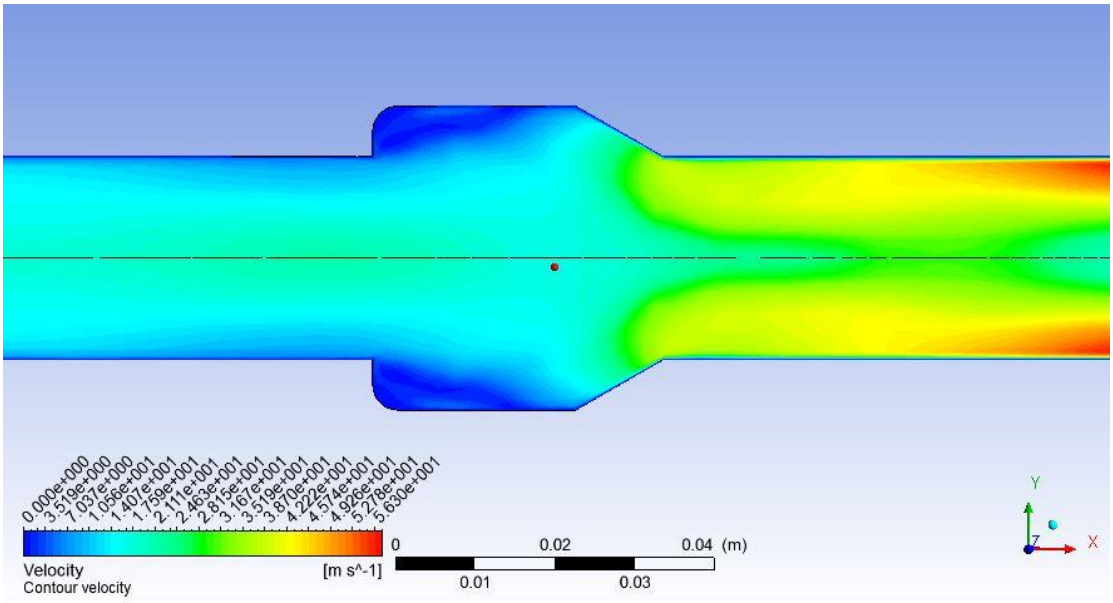

Figure 4-26 Contours of velocity magnitude

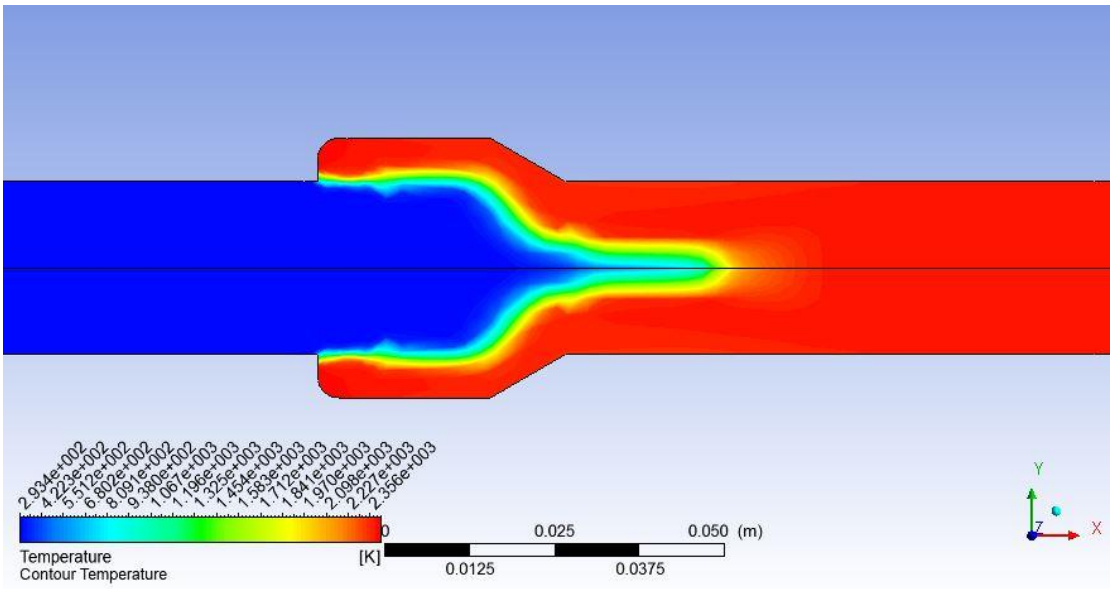

Figure 4-27 Contours of temperature

4.4 Bluff Body Stabilization

Use of co-annular flow in study of diffusion flames is widely used because of its simplicity in design and to include major aspects of diffusion flames. In a co-annular flow of fuel and air, fuel is passed through the inner tube at a certain velocity whereas oxidizer/air is passed through the annular region as shown in figure. The inlet velocity of fuel and air can be varied or kept same. Non-reactive model can be used to study the diffusion phenomenon whereas auto ignited model should be considered for analyzing temperature distribution and burnt species concentration downstream.

Study of bluff body mechanism for flame stabilization for non- premixed flow is presented here. In bluff body stabilized combustion, a non-streamlined body is placed in the flow to produce a recirculating zone downstream. As a result, combustion products settle here to continuously ignite fresh reactants and thus the combustion is self-sustained.

4.4.1 Geometry and flow configuration

The geometry of the combustion chamber is shown in Figure: Geometry/Configuration, where all the units are in mm. The configuration used here is of a hollow cylinder bluff-body stabilized flame investigated at the Sandia National Laboratories and the University of Sydney (Dally et al., 1998).

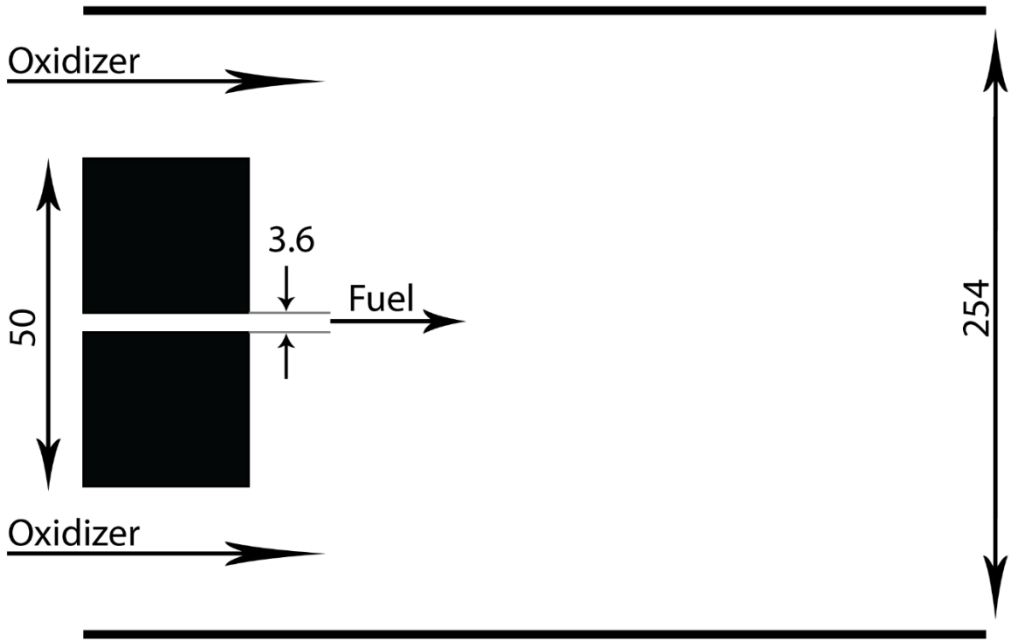

Figure 4-28 Bluff Body Stabilization Configuration

The computational domain is axis symmetric so only a single half of the combustor was modeled. The length of domain was taken as 0.65 m. Methane was taken as fuel and air as oxidizer. As the mixing of fuel and air is the chemical rate determining parameter in non-premixed turbulent flows, Eddy-Dissipation model was used. A global mechanism was considered rather than detail chemical kinetics to minimize computation time. Steady state solution was achieved for this case. Initial conditions for the case are presented on **(Table 4-5).**

Table 4-5 Inlet Conditions for Bluff Body stabilized flame

Fuel (CH_4)	100 m/s
Oxidizer (Air)	100 m/s
Pressure	1 atm
Temperature	300 K

4.4.2 Result and Discussion

From **(Figure 4-29),** we can clearly see the recirculating zone just after the bluff body wall. Two counter-rotation zones are formed above the axis of combustor. The smaller one is due to the fuel velocity and larger one due to the air flow, as a result two stagnation points along the axis are present. Due to this recirculation, fuel and air get mixed together more efficiently in this zone. The effective distance which flow has to travel is increased as the streamlines are curved and thus the effective length of the combustion chamber can be decreased by the use of bluff body. **(Figure 4-30)** shows plot of methane mass fraction in cold flow along the radial direction at different positions, which presents the mixing nature of the flow. At 0.035 m the variation in mass fraction radially is absent, this suggests that complete mixing is achieved at this point. Moreover, the presence of bluff body results in decreasing axial velocity aft of the bluff body wall. So, a region of very low velocity is formed here as shown in **(Figure 4-31)**.

Due to comparatively lower velocity along the axis of the combustor and almost stagnant flow just behind the bluff body, flame stabilization is achieved in this region and the flame seems to be anchored at the bluff body wall, shown in **(Figure 4-32)**. The streamlines near the fuel inlet are circulating, thus flow inside in these stream tubes have sufficient time for combustion compared with the flow far beyond the bluff body, where streamlines are rather straight. Temperature at 4 streamlines shown in **(Figure 4-33)** are

plotted in **(Figure 4-34)**. Here temperature in streamlines near fuel inlet rapidly increases and the temperature on streamlines far beyond bluff body is unaffected due to absence of fuel.

Various detailed mechanism for methane combustion give slightly different value of adiabatic flame temperature. So for stoichiometric air fuel ratio a range of 2300 – 2400 K is reasonable adiabatic flame temperature. From the case analysis, highest temperature achieved was found to be 2395 K. At exit, highest temperature is found only at the center of the combustor. The mixing of comparatively colder air and exhaust gas can be done to minimize overall exit temperature. Use of swirler and/or other mixing enhancement techniques can also done for this purpose. As mixing governs the rate of combustion in non-premixed flows various mixing enhancement techniques can also be used to minimize the length of combustor for non-premixed flows.

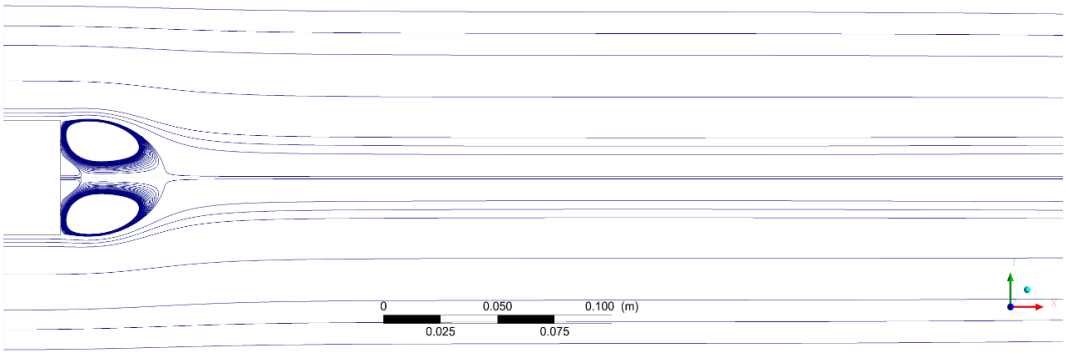

Figure 4-29 Streamlines in cold flow

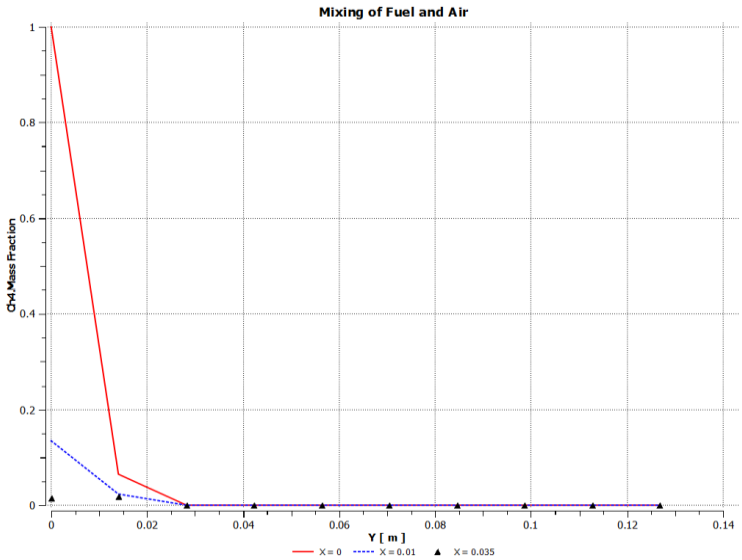

Figure 4-30 Mass Fraction of Methane in cold flow

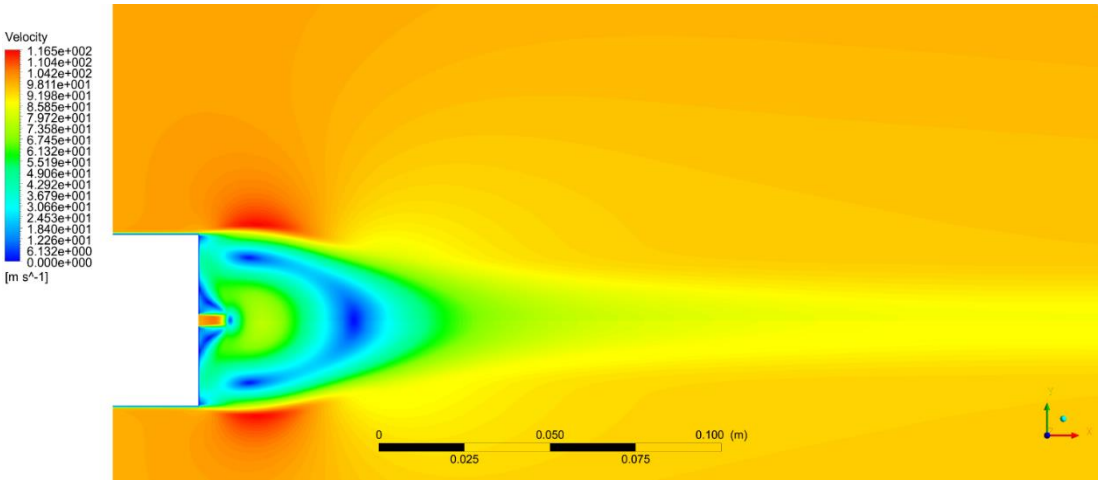

Figure 4-31 Contours of velocity zoomed at fuel inlet in cold flow

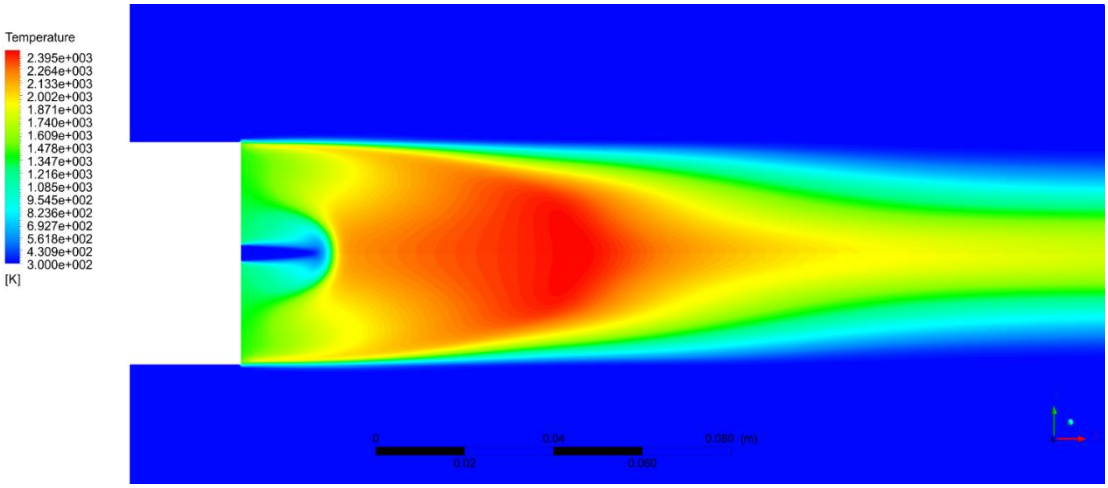

Figure 4-32 Contours of Temperature after combustion, zoomed at fuel inlet

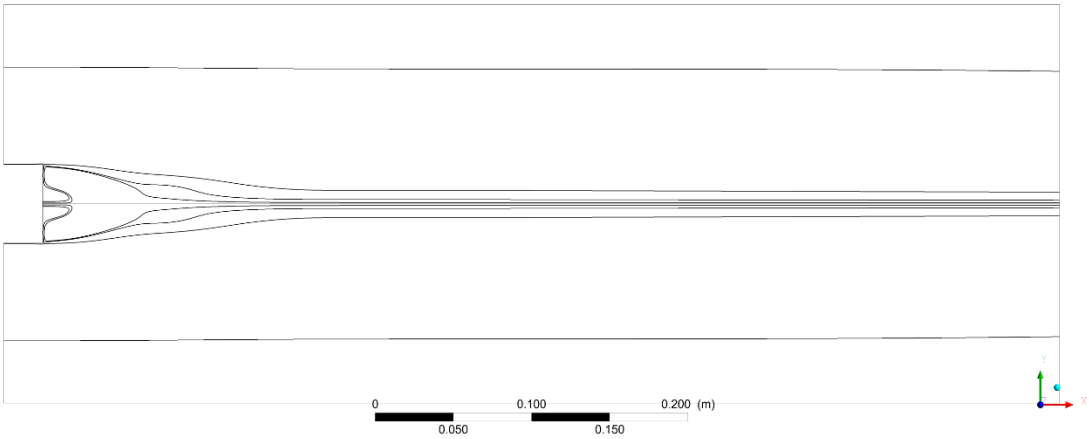

Figure 4-33 Streamlines in reacting flow

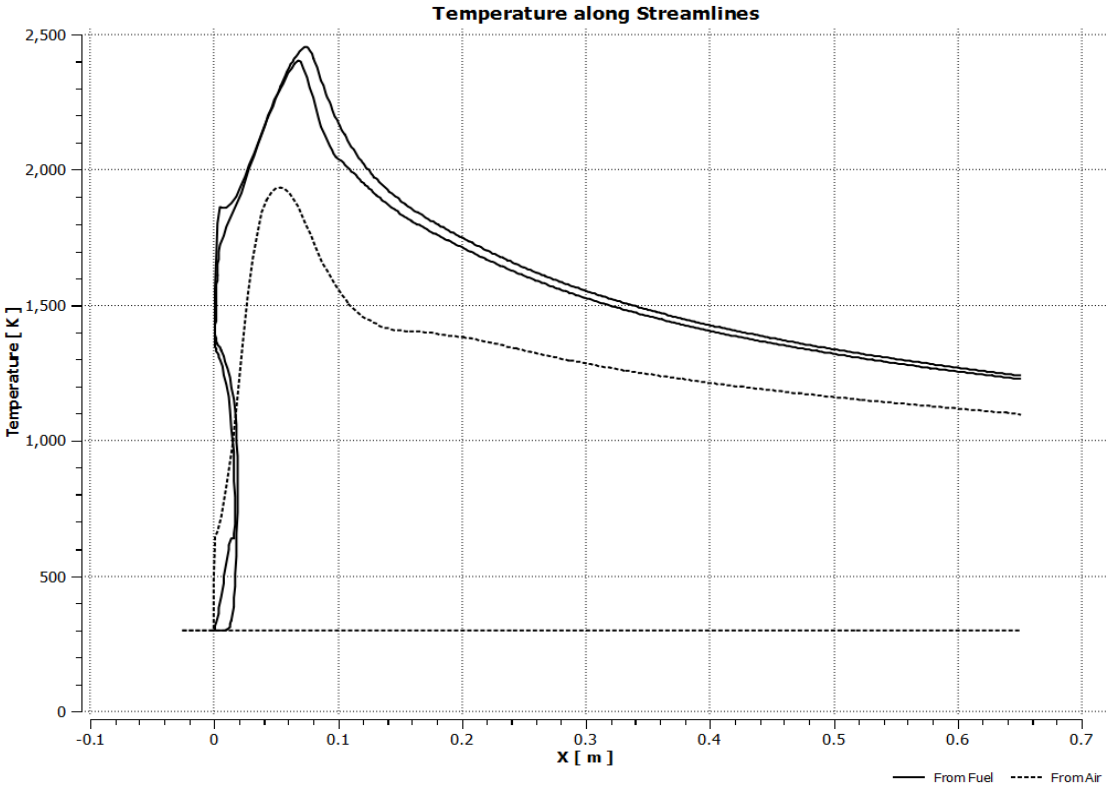

Figure 4-34 Temperature along Streamlines

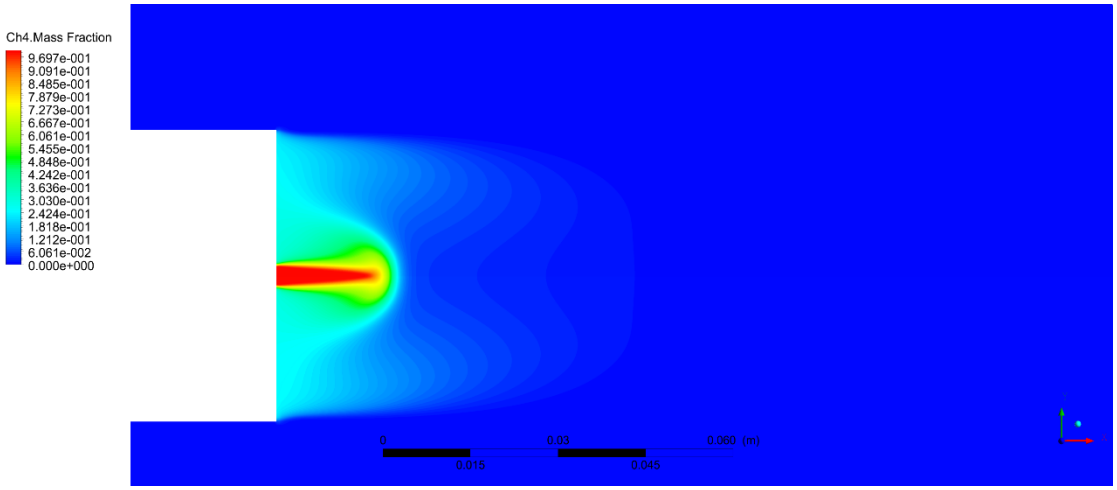

Figure 4-35 Contours of Methane mass fraction after combustion

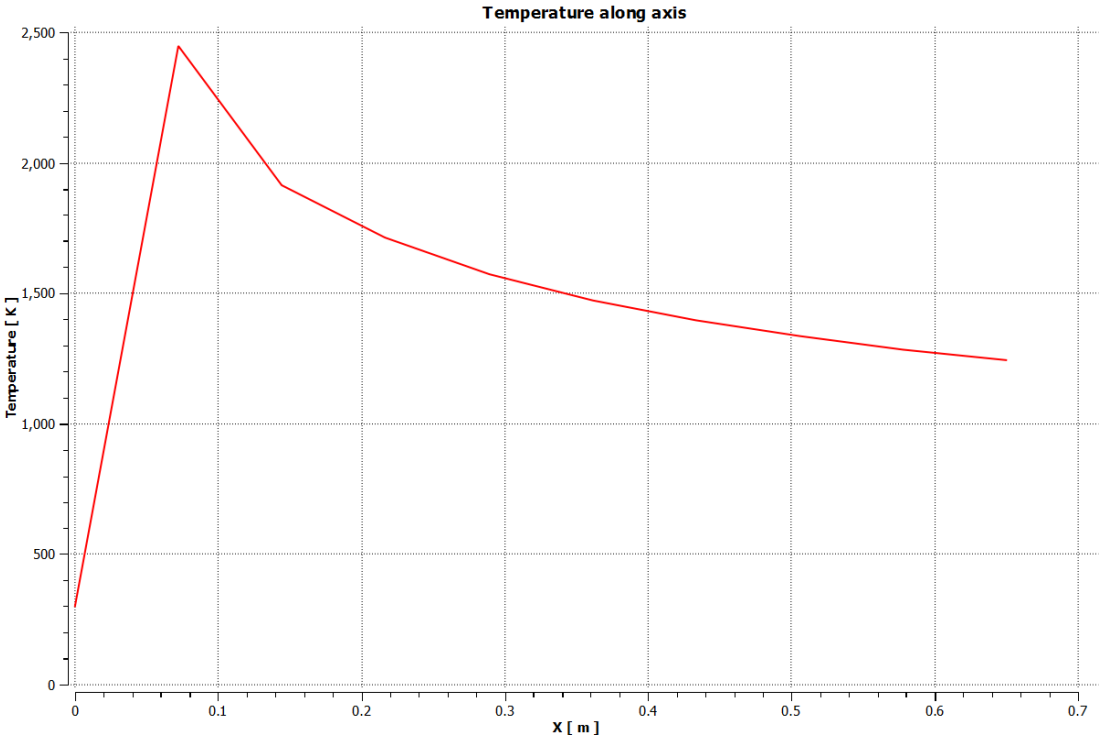

Figure 4-36 Temperature along axis

CONCLUSIONS AND RECOMENDATIONS

5.1 Conclusions

1. The mathematical model for Closed Homogeneous Constant Pressure Reactor (CHCPR) and one-dimensional Premixed Reactive Flow Model (PRFM) was developed.
2. Detailed gas phase kinetics was coupled with thermodynamics and flow properties.
3. The developed solvers were verified for H_2/air finite rate chemistry model consisting of 20 reactions and 9 species.
4. The developed solver can be used to study how species concentration, adiabatic flame temperature, auto-ignition and reaction times are affected by initial temperature, initial pressure, fuel equivalence ratio, presence of foreign species in oxidizer, etc.
5. A preliminary design of gas combustor of 20 kW was done with the help of CHCPR and PRFM solvers and finally simulated in ANSYS Fluent. The mass flow rates, air inlet ports' dimensions and positioning of secondary and dilution air inlet in a gas combustor is studied as a test case. Similar methodology can be used in preliminary design of slender subsonic gas combustion systems.
6. Simulation of bluff body stabilization and cavity flame holder was done in ANSYS Fluent to study the effect of bluff body and cavity on reacting flow.

5.2 Recommendations

1. The solver can be expanded to include the pressure dependence of the reactions.
2. Current developed model can be extended to study the reaction behind shock wave after addition of compressibility effect.
3. Present numerical solver can be modified incorporating adaptive step size, order or both to achieve stable and rapid solution of stiff differential equations for large fuel molecules.
4. Conduction and diffusion can be incorporated in the developed model.
5. Phase change can be considered during reaction.

REFERENCES

Alim, M., & Malalasekera, W. (2009). Transport and chemical kinetics of H_2/N_2 jet flame: A flamelet modelling approach with NOx prediction. *Journal of Naval Architecture and Marine Engineering*, *2*(1). https://doi.org/10.3329/jname.v2i1.2028

Balakrishnan, G., Smooke, M. D., & Williams, F. A. (1995). A numerical investigation of extinction and ignition limits in laminar nonpremixed counterflowing hydrogen-air streams for both elementary and reduced chemistry. *Combustion and Flame*, *102*(3), 329–340. https://doi.org/10.1016/0010-2180(95)00031-Z

Barbe, P., Battin-Leclerc, F., & Côme, G. (1995). Experimental and modelling study of methane and ethane oxidation between 773 and 1573 K. *Journal de Chimie Physique*, *92*, 1666–1692. https://doi.org/10.1051/jcp/1995921666

Basevich, V. Y. (1987). Chemical kinetics in the combustion processes: A detailed kinetics mechanism and its implementation. *Progress in Energy and Combustion Science*. https://doi.org/10.1016/0360-1285(87)90011-6

Basevich, V. Y., Belyaev, a. a., & Frolov, S. M. (2009). Mechanisms of the oxidation and combustion of normal alkanes: Passage from C1-C4 to C2H5. *Russian Journal of Physical Chemistry B*, *3*(4), 629–635. https://doi.org/10.1134/S1990793109040186

Battin-Leclerc, F., Blurock, E., Bounaceur, R., Fournet, R., Glaude, P.-A., Herbinet, O., … Warth, V. (2011). Towards cleaner combustion engines through groundbreaking detailed chemical kinetic models. *Chemical Society Reviews*, *40*(9), 4762–4782. https://doi.org/10.1039/c0cs00207k

Bittker, D. A., & Scullin, V. J. (1972). General chemical kinetics computer program for static and flow reactions, with application to combustion and shock-tube kinetics. Retrieved from https://ntrs.nasa.gov/search.jsp?R=19720007476

Blakley, G. R. (1982). Chemical equation balancing: A general method which is quick, simple, and has unexpected applications. *Journal of Chemical Education*, *59*(9), 728. https://doi.org/10.1021/ed059p728

Brown, P. N., Byrne, G. D., & Hindmarsh, A. C. (2006). VODE: A Variable-Coefficient ODE Solver. *http://dx.doi.org/10.1137/0910062*. https://doi.org/10.1137/0910062

Burcat, a, & Branko, R. (2005). Third millennium ideal gas and condensed phase thermochemical database for combustion with updates from active thermochemical tables. *Technical Report*, *ANL-05/20*(September), ANL-05/20 TAE 960. https://doi.org/10.2172/925269

Chetiyar, J. G. (2015). DESIGN AND IMPROVEMENT OF COMBUSTION CHAMBER FOR SMALL GAS. *International Conference on Recent Advancement in Mechanical Enginnering {&}technology*, (9), 287–293. Retrieved from www.jchps.com

Dally, B. B., Fletcher, D. F., & Masri, A. R. (1998). Flow and mixing fields of turbulent bluff-body jets and flames. *Combustion Theory and Modelling*, *2*(2), 193–219. https://doi.org/10.1088/1364-7830/2/2/006

Date, A. W. (2011). *Analytic Combustion: With Thermodynamics, Chemical Kinetics and Mass Transfer*. Cambridge University Press. https://doi.org/10.1017/CBO9780511976759

Erickson, W. D., & Klick, G. F. (1970). Analytical chemical kinetic study of the effect of carbon dioxide and water vapor on hydrogen-air constant-pressure combustion. Retrieved from https://ntrs.nasa.gov/search.jsp?R=19700014243

Goodwin, D., Moffat, H., & Speth, R. (2016, January). Cantera: An object-oriented software toolkit for chemical kinetics, thermodynamics, and transport processes. https://doi.org/10.5281/zenodo.170284

Gordon, S., & McBride, B. J. (1971). Computer program for calculation of complex chemical equilibrium compositions rocket performance incident and reflected shocks, and Chapman-Jouguet detonations. *Computer Program for Calculation of Complex Chemical Equilibrium Compositions Rocket Performance Incident and Reflected Shocks and ChapmanJouguet Detonations*, 250.

Hajitaheri, S. (2012). Design Optimization and Combustion Simulation of Two Gaseous and Liquid-Fired Combustors. Retrieved from https://uwspace.uwaterloo.ca/handle/10012/6730

Hersch, M. (1967). Hydrogen-oxygen Chemical Reaction Kinetics in Rocket Engine Combustion. Retrieved from http://ntrs.nasa.gov/search.jsp?R=19680002174

Hindmarsh, A. C. (1980). LSODE and LSODI, two new initial value ordinary differnetial equation solvers. *ACM SIGNUM Newsletter*, *15*(4), 10–11. https://doi.org/10.1145/1218052.1218054

IEA. (2014). *Key World Energy Statistics 2014*.

Jelezniak, M., Jelezniak, I., & Distance, A. (2008). Use of Chemked for Simulation of Gas-Phase Chemical Reactors. *Reactions*, (April), 1–17. Retrieved from http://www.chemked.com/,

Jensen, J. T. (2011). Minimum Ignition Energy in a Hygrogen Combustible Mixture, (June). Retrieved from http://www.pvv.ntnu.no/%7B~%7Dnilshau/studenter/jensen.pdf

Kee, R. J., Rupley, F. M., Meeks, E., & Miller, J. a. (1996). Chemkin-III: a fortran chemical kinetics package for the analysis of gas- phase chemical and plasma kinetics. *Work*, (May), 3–164. https://doi.org/10.2172/481621

Kee, R. J., Rupley, F. M., Meeks, E., & Miller, J. A. (1996). CHEMKIN-III: A FORTRAN CHEMICAL KINETICS PACKAGE FOR THE ANALYSIS OF GAS-PHASE CHEMICAL AND PLASMA KINETICS. Retrieved from http://200.17.228.88/CFD/bibliografia/propulsao/CHEMKIN_III.pdf

Kee, R. J., Rupley, F. M., & Miller, J. A. (1989). *CHEMKIN-II: A FORTRAN chemical kinetics package for the analysis of gas phase chemical kinetics*. *SANDIA Report No. SAND89-8009B*. https://doi.org/10.2144/000113845

Kumaran, K., & Babu, V. (2009). Investigation of the effect of chemistry models on the numerical predictions of the supersonic combustion of hydrogen. *Combustion and Flame*, *156*(4), 826–841. https://doi.org/10.1016/j.combustflame.2009.01.008

L. W. HUELLMANTEL, R. W. ZIEMER, A. L. I. B. C. (1957). Stabilization of Premixed Propane-Air Flames in Recessed Ducts. *Journal of Jet Propulsion*, *27*(1), 31–34. https://doi.org/10.2514/8.12565

Lieuwen, T., McDonell, V., Santavicca, D., & Sattelmayer, T. (2008). Burner Development and Operability Issues Associated with Steady Flowing Syngas Fired Combustors. *Combustion Science and Technology*, *180*(6), 1169–1192. https://doi.org/10.1080/00102200801963375

Mclain, A. G., & Rao, C. S. R. (1976). A hybrid computer program for rapidly solving flowing or static chemical kinetic problems involving many chemical species. Retrieved from https://ntrs.nasa.gov/search.jsp?R=19760022294

Meredith, K., & Black, D. (2006). Automated Global Mechanism Generation for Use in CFD Simulations. In *44th AIAA Aerospace Sciences Meeting and Exhibit* (pp. 1–13). American Institute of Aeronautics and Astronautics. https://doi.org/10.2514/6.2006-1168

Mott, D. R., & Oran, E. S. (2001). CHEMEQ2: A Solver for the Stiff Ordinary Differential Equations of Chemical Kinetics, 67. Retrieved from http://www.dtic.mil/docs/citations/ADA392490

Nakaya, S., Hatori, K., Tsue, M., Kono, M., Segawa, D., & Kadota, T. (2006). A numerical study on the effect of the equivalence ratio of hydrogen/air or methane/air mixtures on minimum ignition energy in spark ignition process. *Nihon Kikai Gakkai Ronbunshu, B Hen/Transactions of the Japan Society of Mechanical Engineers, Part B*, *72*(3), 818–824. https://doi.org/10.1299/kikaib.72.818

Niemeyer, K. E., Curtis, N. J., & Sung, C. J. (2017). pyJac: Analytical Jacobian generator for chemical kinetics. *Computer Physics Communications*, *215*, 188–203. https://doi.org/10.1016/j.cpc.2017.02.004

Oran, E. S., & Boris, J. P. (1981). Detailed modelling of combustion systems. *Progress in Energy and Combustion Science*. https://doi.org/10.1016/0360-1285(81)90014-9

Petrova, M. V, & Williams, F. A. (2006). A small detailed chemical-kinetic mechanism for hydrocarbon combustion. *Combustion and Flame*, *144*(3), 526–544. https://doi.org/10.1016/j.combustflame.2005.07.016

Petzold, L. R. (1982). A description of Dassl: A differential / algebraic system solver. *Sand828637*.

Radhakrishnan, K. (1994). LSENS - A General Chemical Kinetics and Sensitivity Analysis Code for Homogeneous Gas-Phase Reactions, (1328).

Safta, C., Najm, H. N., & Knio, O. (2011). TChem - A Software Toolkit for the Analysis of Complex Kinetic Models. *Sandia Report*, *SAND2011-3*(May). https://doi.org/10.2172/1113874

Shampine, L. F., & Reichelt, M. W. (1997). The MATLAB ODE Suite. *SIAM Journal on Scientific Computing*, *18*(1), 1–22. https://doi.org/10.1137/S1064827594276424

Simmie, J. M. (2003). Detailed chemical kinetic models for the combustion of hydrocarbon fuels. *Progress in Energy and Combustion Science*. https://doi.org/10.1016/S0360-1285(03)00060-1

UCSD. (2014). Chemical-Kinetic Mechanisms for Combustion Applications.

Westbrook, C. K., Mizobuchi, Y., Poinsot, T. J., Smith, P. J., & Warnatz, J. (2005). Computational combustion. *Proceedings of the Combustion Institute, 30*(1), 125–157. https://doi.org/10.1016/j.proci.2004.08.275

Young, T. R. J. (1980). *CHEMEQ - A Subroutine for Solving Stiff Ordinary Differential Equations*. Retrieved from http://www.dtic.mil/docs/citations/ADA083545

Zhukov, V. P. (2011). Verification, Validation and Testing of Kinetic Mechanisms of Hydrogen Combustion in Fluid Dynamic Computations, (August 2013). https://doi.org/10.5402/2012/475607

APPENDIX A: Reaction Mechanism for Hydrogen Combustion

```
ELEMENTS  H   O   N  END

SPECIES H2  H  O2  O  OH  HO2  H2O2  H2O   N2 END

REACTIONS
H+O2+M=HO2+M                              3.61E17  -0.72       0.
  H2O/18.6/  H2/2.86/
H+H+M=H2+M                                1.0E18   -1.0        0.
H+H+H2=H2+H2                              9.2E16   -0.6        0.
H+H+H2O=H2+H2O                            6.0E19   -1.25       0.
H+OH+M=H2O+M                              1.6E22   -2.0        0.
  H2O/5/
H+O+M=OH+M                                6.2E16   -0.6        0.
  H2O/5/
O+O+M=O2+M                                1.89E13   0.0    -1788.
H2O2+M=OH+OH+M                            1.3E17    0.0    45500.
H2+O2=2OH                                 1.7E13    0.0    47780.
OH+H2=H2O+H                               1.17E9    1.3     3626.
O+OH=O2+H                                 3.61E14  -0.5        0.
O+H2=OH+H                                 5.06E4    2.67    6290.
OH+HO2=H2O+O2                             7.5E12    0.0      0.0
H+HO2=2OH                                 1.4E14    0.0     1073.
O+HO2=O2+OH                               1.4E13    0.0     1073.
2OH=O+H2O                                 6.0E+8    1.3        0.
H+HO2=H2+O2                               1.25E13   0.0        0.
HO2+HO2=H2O2+O2                           2.0E12    0.0        0.
H2O2+H=HO2+H2                             1.6E12    0.0     3800.
H2O2+OH=H2O+HO2                           1.0E13    0.0     1800.
END

GLOBAL
H2+0.5O2+0.5N2=H2O+0.5N2
H2/1/ %%FUEL
O2/0.21/N2/0.79 %%Oxidizer
END
```

Source**:** (Robert J Kee et al., 1996)

APPENDIX B: Thermochemical Data

```
H                 L 6/94H   1    0    0    0G   200.000  6000.000 1000.       1
 0.25000000E+01 0.00000000E+00 0.00000000E+00 0.00000000E+00 0.00000000E+00    2
 0.25473660E+05-0.44668285E+00 0.25000000E+01 0.00000000E+00 0.00000000E+00    3
 0.00000000E+00 0.00000000E+00 0.25473660E+05-0.44668285E+00 0.26219035E+05    4
H2  REF ELEMENT   T 2/17H  2.   0.   0.   0.G   200.000  6000.000 1000.       1
 2.98711895E+00 7.36069465E-04-9.00982609E-08-7.41224720E-13 6.58618037E-16    2
-8.35448659E+02-1.33268877E+00 3.50207268E+00 8.65475654E-05-2.63683344E-07    3
 3.37306621E-10-2.92359706E-14-1.04631279E+03-4.25875759E+00 0.00000000E+00    4
N                 L 6/88N   1    0    0    0G   200.000  6000.000 1000.       1
 0.24159429E+01 0.17489065E-03-0.11902369E-06 0.30226244E-10-0.20360983E-14    2
 0.56133775E+05 0.46496095E+01 0.25000000E+01 0.00000000E+00 0.00000000E+00    3
 0.00000000E+00 0.00000000E+00 0.56104638E+05 0.41939088E+01 0.56850013E+05    4
N2 REF ELEMENT    G 8/02N  2.   0.   0.   0.G   200.000  6000.000 1000.       1
 2.95257637E+00 1.39690040E-03-4.92631603E-07 7.86010195E-11-4.60755204E-15    2
-9.23948688E+02 5.87188762E+00 3.53100528E+00-1.23660988E-04-5.02999433E-07    3
 2.43530612E-09-1.40881235E-12-1.04697628E+03 2.96747038E+00 0.00000000E+00    4
OH HYDROXYL RADI  IU3/03O  1.H  1.   0.   0.G   200.000  6000.000 1000.       1
 2.83853033E+00 1.10741289E-03-2.94000209E-07 4.20698729E-11-2.42289890E-15    2
 3.69780808E+03 5.84494652E+00 3.99198424E+00-2.40106655E-03 4.61664033E-06    3
-3.87916306E-09 1.36319502E-12 3.36889836E+03-1.03998477E-01 4.48613328E+03    4
HO2               T 1/09H  1.O  2.   0.   0.G   200.000  5000.000 1000.       1
 4.17228741E+00 1.88117627E-03-3.46277286E-07 1.94657549E-11 1.76256905E-16    2
 3.10206839E+01 2.95767672E+00 4.30179807E+00-4.74912097E-03 2.11582905E-05    3
-2.42763914E-08 9.29225225E-12 2.64018485E+02 3.71666220E+00 1.47886045E+03    4
H2O2              T 8/03H  2.O  2.   0.   0.G   200.000  6000.000 1000.       1
 4.57977305E+00 4.05326003E-03-1.29844730E-06 1.98211400E-10-1.13968792E-14    2
-1.80071775E+04 6.64970694E-01 4.31515149E+00-8.47390622E-04 1.76404323E-05    3
-2.26762944E-08 9.08950158E-12-1.77067437E+04 3.27373319E+00-1.63425145E+04    4
H2O               L 5/89H   2O   1    0    0G   200.000  6000.000 1000.       1
 0.26770389E+01 0.29731816E-02-0.77376889E-06 0.94433514E-10-0.42689991E-14    2
-0.29885894E+05 0.68825500E+01 0.41986352E+01-0.20364017E-02 0.65203416E-05    3
-0.54879269E-08 0.17719680E-11-0.30293726E+05-0.84900901E+00-0.29084817E+05    4
O                 L 1/90O   1    0    0    0G   200.000  6000.000 1000.       1
 2.54363697E+00-2.73162486E-05-4.19029520E-09 4.95481845E-12-4.79553694E-16    2
 2.92260120E+04 4.92229457E+00 3.16826710E+00-3.27931884E-03 6.64306396E-06    3
-6.12806624E-09 2.11265971E-12 2.91222592E+04 2.05193346E+00 2.99687009E+04    4
O2 REF ELEMENT    RUS 89O   2    0    0    0G   200.000  6000.000 1000.       1
 3.66096065E+00 6.56365811E-04-1.41149627E-07 2.05797935E-11-1.29913436E-15    2
-1.21597718E+03 3.41536279E+00 3.78245636E+00-2.99673416E-03 9.84730201E-06    3
-9.68129509E-09 3.24372837E-12-1.06394356E+03 3.65767573E+00 0.00000000E+00    4
END
```

Source: (Burcat & Branko, 2005)